Bethe-Salpeter equation at leading order in Coulomb gauge

P. Watson and H. Reinhardt

Institut für Theoretische Physik, Universität Tübingen, Auf der Morgenstelle 14, D-72076 Tübingen, Germany

The Bethe-Salpeter equation and leptonic decay constants for pseudoscalar and vector quark-antiquark mesons with arbitrary quark masses are studied in Coulomb gauge, under a leading order truncation. As input, we use a pure linear rising potential, supplemented by a contact term arising from the conservation of total color charge. It is shown how the equations can be written in terms of manifestly finite functions, despite the infrared singular interaction. The resulting equations are solved numerically. Both the pattern of dynamical chiral symmetry breaking and the leading order heavy quark limit are visible.

I. INTRODUCTION

In the theory of strong interactions, quantum chromodynamics (QCD), there are two outstanding issues of importance: confinement and dynamical chiral symmetry breaking. Both of these phenomena are highly nontrivial and are reflected in the nonperturbative regime of the theory. Perhaps the most naive picture of confinement, at least applied to the quark sector of QCD, is the idea that there exists a linear rising potential between quarks at large separation. If a quark is pulled away from its parent hadron, the energy of the system rises until it is energetically favorable that a quark-antiquark pair is created and forming a new system of two hadrons whose constituents remain hidden from view in the same way as for the original. In momentum space, such a linear rising potential corresponds to a strongly infrared enhanced interaction. In Coulomb gauge, lattice results [1–8] show that the temporal component of the nonperturbative gluon propagator (that mediates the quark-antiquark interaction) indeed exhibits such an infrared enhancement.

The inclusion of an infrared singularity, such as that of the aforementioned temporal gluon propagator, into calculations of finite, physical observables is not trivial. Because the singularity occurs for vanishing momentum, a natural place to investigate would be a nonperturbative, continuum formalism, such as that provided by the Dyson-Schwinger and Bethe-Salpeter equations.[1] The Coulomb gauge Dyson-Schwinger equations for QCD have been derived in both the first and second order formalisms (see Refs. [17–19] and references therein) and various aspects explored, such as the one-loop perturbative behavior [18–20], the Slavnov-Taylor identities [21] and the emergence of a nonlocal constraint on the total color charge [22]. Additionally, the case of heavy quarks in the rest frame has also been studied [23–25]. These latter studies show that in the absence of pure Yang-Mills corrections,

the Coulomb gauge rest frame heavy quark limit (where pair creation is absent, such that the linear rising potential remains valid at very large separations) is described precisely by an interaction consisting of single exchange of a temporal gluon. The infrared singularity associated with this interaction is cancelled only when considering color singlet (meson or baryon) bound states, otherwise the objects (propagators or color nonsinglet states) are unphysical.

The issue of dynamical chiral symmetry breaking was studied in Coulomb gauge many years ago (see, for example Refs. [26–28]). It was found that with an infrared enhanced temporal gluon interaction, chiral symmetry breaking does occur, although the chiral condensate and pion leptonic decay constant are too small (it has been demonstrated that the coupling of the quarks to transverse spatial gluons results in a significantly larger condensate [29]). Recently, it has been shown that the twin limits of the chiral and heavy quark propagator in Coulomb gauge, with an infrared enhanced interaction, can be accommodated within a single leading order truncation scheme for the Dyson-Schwinger equations [30].[2] The truncation scheme is centered around an Ansatz for the Coulomb kernel occurring in the action: this term originates from the resolution of Gauss' law and is responsible for the temporal component of the interaction between color charges, i.e., it is intimately connected to the temporal component of the gluon propagator. The interaction between quarks and the spatial components of the gluon field, the three-, and the four-gluon vertices are all neglected under this leading order truncation scheme.

In this paper, the truncation scheme considered in Ref. [30] is extended to the quark-antiquark Bethe-Salpeter equation for pseudoscalar and vector mesons. The primary aim of this study is to show how the infrared singular interaction may be consistently included into the formalism in such a way that physical quantities (meson

---

[1]An alternative approach is to consider the Coulomb gauge Hamiltonian: see for example, Refs. [9–16] and references therein.

[2]The interplay of the chiral and heavy quark symmetries has also been studied in an extended Nambu-Jona-Lasino model [31].

masses and leptonic decay constants with arbitrary quark mass configurations) remain finite. Given that both dynamical chiral symmetry breaking and the heavy quark limit are qualitatively (if not quantitatively) present in the quark propagator under this truncation, the corresponding signals for the meson spectrum will be investigated, both analytically and numerically. As input, the interaction corresponding to a pure linear rising potential will be used, although it is recognized that this is an over-simplification from the physical standpoint.

The paper is organized as follows. In the next section, we shall briefly review the quark propagator under the leading order Coulomb gauge truncation scheme. Section III then goes on to discuss the axialvector Ward-Takahashi identity within the context of Coulomb gauge and in the rest frame. The Bethe-Salpeter equation and leptonic decay constant for pseudoscalar mesons will then be discussed in Sec. IV, with particular emphasis on how the infrared divergence of the interaction can be rendered finite. In Sec. V, the process will be repeated for vector mesons. After briefly discussing the numerical implementation of the equations in Sec. VI, the results will be presented in Sec. VII. We finish with a summary and conclusions.

II. QUARK GAP EQUATION

The central input into the Bethe-Salpeter equation for quark-antiquark mesons stems from the quark propagator and the interaction between the quarks. Let us thus begin by briefly reviewing some pertinent results for the quark propagator obtained previously under the leading order Coulomb gauge truncation scheme that will form the basis for this study [30]. These results incorporate both dynamical chiral symmetry breaking and the heavy quark limit.

The leading order truncation scheme is based on the following instantaneous interaction term in the Coulomb gauge action:

$$S \sim \int dx dy \left[-\frac{1}{2} \rho_x^a \tilde{F}^{ab}(\vec{x}, \vec{y}) \delta(x_0 - y_0) \rho_y^b \right], \quad (2.1)$$

where ρ^a is the color charge (superscript a denotes here the color index in the adjoint representation) associated with the fields. In this case we are interested only in the quark component,

$$\rho_x^a = g \bar{q}_x \gamma^0 T^a q_x, \quad (2.2)$$

with (conjugate) quark field at position x denoted by $(\bar{q}_x)$ q_x, coupling g, and color matrix T^a (Hermitian generator of the $SU(N_c)$ group). In this study, we shall consider an interaction (color diagonal, and in momentum space) of the form

$$g^2 C_F \tilde{F}(\vec{q}) = \mathcal{C}(2\pi)^3 \delta(\vec{q}) + \frac{8\pi\sigma}{(\vec{q}^2)^2} \quad (2.3)$$

($C_F = (N_c^2 - 1)/2N_c$ is the color factor associated with the quarks). Notice that since the interaction vanishes faster

than $1/\vec{q}^2$ in the ultraviolet (UV), there will be no need to consider the renormalization of any quantities and we can omit any discussion of the renormalization constants. The first term of the interaction arises from total color charge conservation (see Refs. [22,30] for a detailed explanation): the constant $\mathcal{C}$ is considered finite until the end of the calculation, whereupon we take the limit $\mathcal{C} \to \infty$. Physically, $\mathcal{C}$ can be thought of as an infinite shift in the potential connected to the fact that one requires an infinite amount of energy to create a color nonsinglet, such as a single quark or gluon, from the vacuum (see later). The second term is strongly infrared (IR) divergent with a coefficient σ. The quark-antiquark potential, derived in the Coulomb gauge heavy quark limit and neglecting the contribution of pure Yang-Mills vertices [23,30] reads, for spatial separation r,

$$V(r) = g^2 C_F \int d\vec{q} \, \tilde{F}(\vec{q})(1 - e^{i\vec{q}\cdot\vec{r}}) = \sigma r, \quad (2.4)$$

where $d\vec{q} = d\vec{q}/(2\pi)^3$. The coefficient σ can be identified as the string tension associated with a purely linear rising potential. The specific value of σ will not be of primary concern in this study because within the context of the leading order truncation scheme it will suffice that all dimensionfull quantities may be expressed in appropriate units of σ, such that the cancellation of the infrared singularities may be demonstrated. As will be seen in Sec. VII, the quantitative results arising from the above potential do not lend themselves to a detailed phenomenological study (this would require a more sophisticated truncation scheme beyond leading order, such as in Ref. [29]). However, we should specify some value for σ in order to make a comparison to physical quantities. The expectation value of $\tilde{F}$ is given by the instantaneous part of the temporal gluon propagator [30,32] and the string tension associated with the coefficient of the infrared divergence is called the Coulomb string tension (σ_c). Thus, we should use $\sigma = \sigma_c$ as input. It is known that σ_c is equal to or larger than the physical Wilson string tension (σ_W) [33] and lattice results indicate that σ_c may be up to ~3 times larger than σ_W [1–3]. At the same time though, it will also be useful to compare with the earlier studies of Refs. [26–28] where σ_W was used. In light of these considerations, we shall consider the range $\sqrt{\sigma} \sim 440$–762 MeV (the lower value corresponding to $\sqrt{\sigma_W}$ and the upper value to $\sqrt{3\sigma_W}$) to give an estimate for the input scale.

Let us now turn to the quark propagator. With the interaction, Eq. (2.1), and under the (leading order) truncation scheme to include only one loop terms, we have the following Dyson-Schwinger equation (in momentum space) for the quark two-point proper function, $\Gamma_{\bar{q}q}$ [30]:

$$\Gamma_{\bar{q}q}(p) = i[\gamma^0 p_0 - \vec{\gamma} \cdot \vec{p} - m]$$
$$+ i g^2 C_F \int d\vec{k} \tilde{F}(\vec{p} - \vec{k}) \gamma^0 W_{\bar{q}q}(k) \gamma^0, \quad (2.5)$$

where m is the bare quark mass and $đk = d^4k/(2\pi)^4$. $\Gamma_{\bar{q}q}$ can be written in terms of two scalar dressing functions A_p and B_p (the subscript p denotes the spatial momentum dependence):

$$\Gamma_{\bar{q}q}(p) = \iota[\gamma^0 p_0 - \vec{\gamma} \cdot \vec{p} A_p - B_p]. \qquad (2.6)$$

The corresponding quark propagator, $W_{\bar{q}q}(p)$ is

$$W_{\bar{q}q}(p) = \frac{(-\iota)}{\Delta_f(p)}[\gamma^0 p_0 - \vec{\gamma} \cdot \vec{p} A_p + B_p],$$
$$\Delta_f(p) = p_0^2 - \vec{p}^2 A_p^2 - B_p^2 + \iota 0_+. \qquad (2.7)$$

Notice that the energy dependence of both the proper two-point function and the propagator is trivial. This arises from the instantaneous character of the interaction and means that the dressing functions (A and B) are independent of the energy p_0. This will lead to important simplifications in the Bethe-Salpeter equation. A possible fourth Dirac structure, proportional to $\gamma^0 p_0 \vec{\gamma} \cdot \vec{p}$ and arising in the noncovariant Coulomb gauge context does not appear, just as in the perturbative case [19].

The static quark propagator is defined as

$$W_{\bar{q}q}^{(s)}(\vec{p}) = \int \frac{dp^0}{2\pi} W_{\bar{q}q}(p) = \frac{\vec{\gamma} \cdot \vec{p} - M_p}{2\omega_p}, \qquad (2.8)$$

where we define the quark mass function, M_p, and quasi-particle energy, ω_p:

$$M_p = \frac{B_p}{A_p}, \qquad \omega_p = \sqrt{\vec{p}^2 + M_p^2}. \qquad (2.9)$$

In the chiral limit, the quark condensate can be defined as (trace over Dirac matrices)

$$\langle \bar{q}q \rangle = N_c \int đ\vec{p} \, \mathrm{Tr}_d W_{\bar{q}q}^{(s)}(\vec{p}) = -2N_c \int đ\vec{p} \frac{M_p}{\omega_p}. \qquad (2.10)$$

The meaning of the quark mass function becomes clear when one considers the quark Dyson-Schwinger equation in the context of the interaction specified in Eq. (2.3). In terms of the dressing functions, A and B, Eq. (2.5) decomposes to

$$A_p = 1 + \frac{1}{2} g^2 C_F \int \frac{đ\vec{k} \, \tilde{F}(\vec{p} - \vec{k})}{\omega_k} \frac{\vec{p} \cdot \vec{k}}{\vec{p}^2}, \qquad (2.11)$$

$$B_p = m + \frac{1}{2} g^2 C_F \int \frac{đ\vec{k} \, \tilde{F}(\vec{p} - \vec{k})}{\omega_k} M_k, \qquad (2.12)$$

whereas combining the two equations in terms of the mass function leads to the Adler-Davis gap equation [27]:

$$M_p = m + \frac{1}{2} g^2 C_F \int \frac{đ\vec{k} \, \tilde{F}(\vec{p} - \vec{k})}{\omega_k} \left[M_k - \frac{\vec{p} \cdot \vec{k}}{\vec{p}^2} M_p \right]. \qquad (2.13)$$

Given that the interaction $\tilde{F}$ contains both the divergent coefficient $\mathcal{C}$ multiplying the δ-function and the IR singular component, A and B are both divergent quantities. However, the integrand of the gap equation contains exactly the cancellation necessary to ensure that the ratio of A and B, namely, the quark mass function M, is finite. The chiral condensate is also finite (see also Sec. VII). Considering the quark proper two-point function written in terms of the self-energy, Σ,

$$\Gamma_{\bar{q}q}(p) = \iota[\gamma^0 p_0 - \vec{\gamma} \cdot \vec{p} - m_q] + \Sigma(\vec{p}), \qquad (2.14)$$

the divergence inherent to the dressing functions A and B has the obvious interpretation of shifting the pole of the full quark propagator to infinity such that one would require infinite energy to excite a single quark from the vacuum. The dynamical content of the quark propagator is contained within the finite mass function and we shall see that in the end, only the mass function (and associated quasiparticle energy) enters the Bethe-Salpeter equation for color-singlet mesons.

A detailed numerical solution to Eq. (2.13) for a range of quark masses was presented in Ref. [30]. Two aspects will be of relevance to this study and for the convenience of the reader, we briefly repeat them here. The mass function is plotted (in appropriate units of the string tension, σ) in the left panel of Fig. 1. One can see that in the chiral case ($m = 0$) the quark mass function is nonzero, signaling the presence of dynamical chiral symmetry breaking. In the right panel of Fig. 1, the dressing ($M - m$) is plotted.
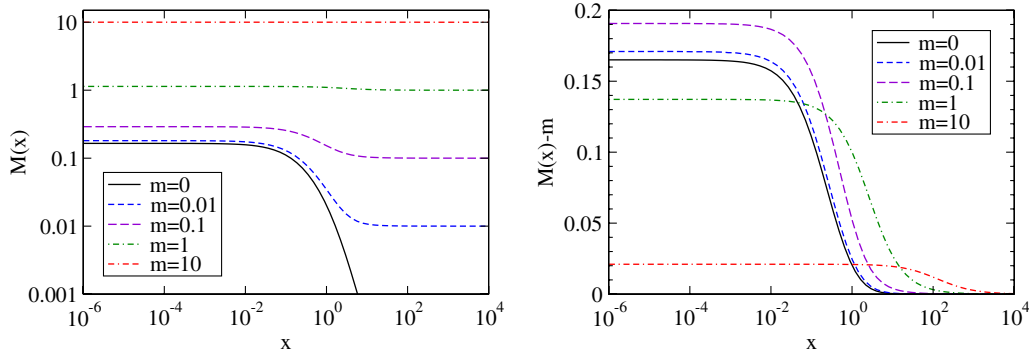

FIG. 1 (color online). [left panel] Quark mass function, $M(x)$, and [right panel] dressing, $M(x) - m$, plotted as functions of $x = \vec{p}^2$ for a range of quark masses. All dimensionfull quantities are in appropriate units of the string tension, σ. See text for details.

As the bare quark mass, m, increases, the dressing initially increases but for larger m starts to decrease. In the (heavy quark) limit $m \to \infty$, one sees that $M \to m$. The original derivation of Eq. (2.13) [27] arose from considering the chiral quark limit. However, with the results for arbitrary quark masses it was shown [30] that the same equation reproduces the rest frame Coulomb gauge heavy quark limit (in the absence of pure Yang-Mills contributions) [23]. Namely, the leading order truncation considered here encompasses both chiral and heavy quark physics.

III. AXIALVECTOR WARD-TAKAHASHI IDENTITY

As is well understood, the pion can be regarded as the Goldstone boson of chiral symmetry breaking. Considering a chiral rotation of the quark field,

$$q_x \to \exp\left\{-\imath \alpha^a \frac{\tau^a}{2} \gamma^5\right\} q_x, \qquad (3.1)$$

where the α^a parametrize the rotation and the τ^a are the Pauli matrices corresponding to a two-flavor system ($a = 1, 2, 3$), the pion vertex may be defined via the (chiral) quark self-energy as

$$\tau^a \Gamma_\pi(\vec{p}) = -\imath \frac{d}{d\alpha^a}\left[\exp\left\{\imath \alpha^b \frac{\tau^b}{2}\gamma^5\right\}\right.$$
$$\times \Sigma(\vec{p}) \exp\left\{\imath \alpha^c \frac{\tau^c}{2}\gamma^5\right\}\Big]_{\alpha^a=0}$$
$$= \frac{\tau^a}{2}\{\gamma^5, \Sigma(\vec{p})\}. \qquad (3.2)$$

Such an approach was used to construct the pion Bethe-Salpeter equation in, for example, Ref. [26]. More generally, the connection between the quark gap equation and the Bethe-Salpeter equation for quark-antiquark bound states is expressed via the axialvector Ward-Takahashi identity (AXWTI). In Coulomb gauge and in the chiral limit, the AXWTI was applied in, for example, Ref. [27]. Here, we are interested in finite, arbitrary mass quarks and the leptonic decay constants, so we shall closely follow the approach of Ref. [34]. There, the context was the consideration of covariant gauges. Here, for the convenience of the reader, we shall repeat their argumentation for Coulomb gauge in the rest frame and specifically within our leading order truncation scheme.

Splitting the energy and spatial momentum arguments of the (noncovariant) propagators and proper functions, so that, for example, $\Gamma_{\bar{q}q}(p) = \Gamma_{\bar{q}q}(p^0, \vec{p})$, let us consider the following combination (the energy and spatial momentum dependence of Λ will be explained below):

$$\Lambda^{a5}(\vec{p}; p^0, P^0) = \Gamma^+_{\bar{q}q}(p^0 + P^0/2, \vec{p})\gamma^5\frac{\tau^a}{2}$$
$$+ \gamma^5\frac{\tau^a}{2}\Gamma^-_{\bar{q}q}(p^0 - P^0/2, \vec{p}), \qquad (3.3)$$

where the two quark proper two-point functions, $\Gamma^\pm_{\bar{q}q}$, have arbitrary bare masses $m^\pm$ and correspondingly, different

dressing functions $A^\pm$, $B^\pm$ and $M^\pm$. Using the quark Dyson-Schwinger equation, Eq. (2.5), to rewrite the proper two-point functions, one obtains after some straightforward manipulation

$$\Lambda^{a5}(\vec{p}; p^0, P^0)$$
$$= -\imath\gamma^5[P^0\gamma^0 + (m^+ + m^-)]\frac{\tau^a}{2} - \imath g^2 C_F \int \dbar k \tilde{F}(\vec{p}-\vec{k})$$
$$\times \gamma^0 W^+_{\bar{q}q}(k^0 + P^0/2, \vec{k})\Lambda^{a5}(\vec{k}; k^0, P^0)W^-_{\bar{q}q}(k^0 - P^0/2, \vec{k})\gamma^0. \qquad (3.4)$$

We immediately notice that the above is a truncated Dyson-Schwinger (or inhomogeneous Bethe-Salpeter) equation for a generalized quark-antiquark, color-singlet vertex Λ^{a5}. Given that the right-hand side expression is independent of the energy p^0, Λ^{a5} is also independent of p^0 and this arises because of the instantaneous character of the interaction. The energy P^0 is the total energy flowing through the quark-antiquark pair, whereas the spatial momentum $\vec{p}$ (or $\vec{k}$ within the integral) flows along the quark line. The vertex is thus in the rest frame of the quark-antiquark pair and this shall be extremely useful in our analysis. It is convenient to use the shorthand notation $k^\pm$ to denote the energy and spatial momentum arguments $(k^0 \pm P^0/2, \vec{k})$ (similarly for $p^\pm$) such that the above equation reads

$$\Lambda^{a5}(\vec{p}; P^0) = -\imath\gamma^5[P^0\gamma^0 + (m^+ + m^-)]\frac{\tau^a}{2}$$
$$- \imath g^2 C_F \int \dbar k \tilde{F}(\vec{p}-\vec{k})\gamma^0 W^+_{\bar{q}q}(k^+)$$
$$\times \Lambda^{a5}(\vec{k}; P^0)W^-_{\bar{q}q}(k^-)\gamma^0. \qquad (3.5)$$

The axialvector Ward-Takahashi identity tells us that this generalized vertex can be rewritten as

$$\Lambda^{a5}(\vec{p}; P^0) = -\imath P^0\Gamma^{a5}_0(\vec{p}; P^0) - \imath(m^+ + m^-)\Gamma^{a5}(\vec{p}; P^0), \qquad (3.6)$$

where Γ^{a5}_0 and Γ^{a5} are the temporal component of the axialvector vertex function and the pseudoscalar vertex function, respectively (both in the rest frame). Separating the temporal axialvector and pseudoscalar components of Λ^{a5} in Eq. (3.5), one can write down the Dyson-Schwinger equations for Γ^{a5}_0 and Γ^{a5}:

$$\Gamma^{a5}_0(\vec{p}; P^0)$$
$$= \gamma^5\gamma^0\frac{\tau^a}{2} - \imath g^2 C_F \int \dbar k \tilde{F}(\vec{p}-\vec{k})\gamma^0 W^+_{\bar{q}q}(k^+)\Gamma^{a5}_0(\vec{k}; P^0)$$
$$\times W^-_{\bar{q}q}(k^-)\gamma^0, \qquad (3.7)$$

$$\Gamma^{a5}(\vec{p}; P^0) = \gamma^5\frac{\tau^a}{2} - \imath g^2 C_F \int \dbar k \tilde{F}(\vec{p}-\vec{k})\gamma^0 W^+_{\bar{q}q}(k^+)$$
$$\times \Gamma^{a5}(\vec{k}; P^0)W^-_{\bar{q}q}(k^-)\gamma^0. \qquad (3.8)$$

Notice that both of these equations hold for arbitrary total energy P^0, i.e., they are not at resonance.

Now let us consider the homogeneous Bethe-Salpeter equation in the pseudoscalar channel. Taking Eq. (3.8) and making the Ansatz that Γ^{a5} has a simple pole (in the rest frame and with the quantum numbers of a pseudoscalar vertex) with an as yet unknown residue, r_{PS}, of the form

$$\Gamma^{a5}(\vec{p}; P^0) = \frac{r_{PS}}{P_0^2 - M_{PS}^2} \Gamma_{PS}^a(\vec{p}; P^0) + \text{non-res.}, \quad (3.9)$$

(with finite parts denoted 'non-res.') then, at resonance, one has the homogeneous Bethe-Salpeter equation:

$$\Gamma_{PS}^a(\vec{p}; P^0) \overset{P_0^2 = M_{PS}^2}{=} -\imath g^2 C_F \int \dbar k \tilde{F}(\vec{p} - \vec{k}) \gamma^0 W_{\bar{q}q}^+(k^+)$$
$$\times \Gamma_{PS}^a(\vec{k}; P^0) W_{\bar{q}q}^-(k^-) \gamma^0. \quad (3.10)$$

Alternatively, taking Eq. (3.7) and making instead the Ansatz that

$$\Gamma_0^{a5}(\vec{p}; P^0) = \frac{r_{AV} P^0}{P_0^2 - M_{PS}^2} \Gamma_{PS}^a(\vec{p}; P^0) + \text{non-res.}, \quad (3.11)$$

one arrives at the identical homogeneous equation. Combining Eqs. (3.9) and (3.11) and inserting into the AXWTI, Eq. (3.6), one also has that

$$\Lambda^{a5}(\vec{p}; P^0) = -\imath [r_{AV} M_{PS}^2 + r_{PS}(m^+ + m^-)] \frac{\Gamma_{PS}^a(\vec{p}; P^0)}{P_0^2 - M_{PS}^2}$$
$$+ \text{non-res.} \quad (3.12)$$

Given the definition of Λ^{a5}, Eq. (3.3), and knowing that the quark proper two-point function contains no resonant components, the unknown residues r_{PS} and r_{AV} must obey the relation

$$r_{AV} M_{PS}^2 = -r_{PS}(m^+ + m^-). \quad (3.13)$$

To obtain more information about the residues, some manipulation of the kernel is required. Replacing the Dirac (and trivial flavor) indices and denoting the Bethe-Salpeter kernel K such that

$$K_{\alpha\gamma;\delta\beta}(\vec{p}, \vec{k}) = \imath g^2 C_F \tilde{F}(\vec{p} - \vec{k}) [\gamma^0]_{\alpha\gamma} [\gamma^0]_{\delta\beta}, \quad (3.14)$$

Eq. (3.8) can be written as

$$\Gamma_{\alpha\beta}^{a5}(\vec{p}; P^0) = \left[\gamma^5 \frac{\tau^a}{2} \right]_{\alpha\beta} - \int \dbar k K_{\alpha\gamma;\delta\beta}(\vec{p}, \vec{k})$$
$$\times [W_{\bar{q}q}^+(k^+) \Gamma^{a5}(\vec{k}; P^0) W_{\bar{q}q}^-(k^-)]_{\gamma\delta}, \quad (3.15)$$

with a similar form for Eq. (3.7). Equation (3.15) is represented diagrammatically in the top line of Fig. 2. The equation can be recursively expanded to an infinite series in the kernel as shown in the second line of Fig. 2. One sees that this has the effect of replacing the non-perturbative Bethe-Salpeter vertex (Γ^{a5}) within the
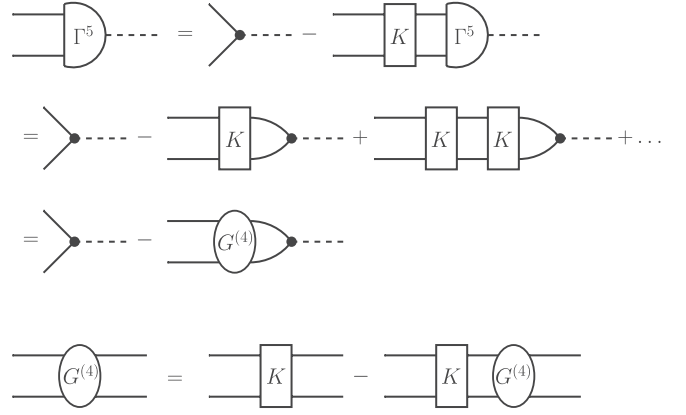

FIG. 2. [top line] Diagrammatic representation of Eq. (3.15) in terms of the Bethe-Salpeter kernel, K, [second line] expanded as a series in K and [third line] the equivalent expression in terms of the amputated four-point function $G^{(4)}$. [fourth line] The equation for $G^{(4)}$ (which can be also understood via the expansion in terms of K). Internal lines denote dressed quark propagators, the dot denotes the tree-level vertex. See text for details.

integral with the tree-level term ($\gamma^5 \tau^a / 2$) and an infinite series in terms of the kernel (K). With the form of the kernel under consideration here, Eq. (3.14), this is nothing other than the ladder resummation of the Bethe-Salpeter equation. However, it is also known that the ladder resummation is directly connected to the amputated connected four-point quark-antiquark Green's function, $G^{(4)}$ (studied explicitly within the context of heavy quarks in the Coulomb gauge rest frame and with the same truncation scheme in Ref. [25]). The equation for $G^{(4)}$ is shown diagrammatically in the last line of Fig. 2. Replacing then the infinite ladder series with $G^{(4)}$ in the equation for Γ^{a5} gives the third line of Fig. 2. Equations (3.7) and (3.8) can thus be rewritten as

$$\Gamma_{0\alpha\beta}^{a5}(\vec{p}; P^0) = \left[\gamma^5 \gamma^0 \frac{\tau^a}{2} \right]_{\alpha\beta} - \int \dbar k G_{\alpha\beta;\gamma\delta}^{(4)}(\vec{p}, \vec{k}; P^0)$$
$$\times \left[W_{\bar{q}q}^+(k^+) \gamma^5 \gamma^0 \frac{\tau^a}{2} W_{\bar{q}q}^-(k^-) \right]_{\delta\gamma}, \quad (3.16)$$

$$\Gamma_{\alpha\beta}^{a5}(\vec{p}; P^0) = \left[\gamma^5 \frac{\tau^a}{2} \right]_{\alpha\beta} - \int \dbar k G_{\alpha\beta;\gamma\delta}^{(4)}(\vec{p}, \vec{k}; P^0)$$
$$\times \left[W_{\bar{q}q}^+(k^+) \gamma^5 \frac{\tau^a}{2} W_{\bar{q}q}^-(k^-) \right]_{\delta\gamma}. \quad (3.17)$$

It is explicitly known that in the Coulomb gauge heavy quark limit, $G^{(4)}$ contains (physical) resonant components in the color-singlet channel [25]. In the pseudoscalar channel under consideration here, let us write

$$G^{(4)}_{\alpha\beta;\gamma\delta}(\vec{p}, \vec{k}; P^0) = [\Gamma^b_{PS}(\vec{p}; P^0)]_{\alpha\beta} \frac{(-\iota N)}{P_0^2 - M_{PS}^2}$$
$$\times [\bar{\Gamma}^b_{PS}(\vec{k}; -P^0)]_{\gamma\delta} + \text{non res.,} \quad (3.18)$$

where N is an unspecified normalization constant (we will use $N = 1$ later). The conjugate Bethe-Salpeter vertex function is defined with the aid of the charge conjugation matrix C, such that

$$\bar{\Gamma}^b_{PS}(\vec{k}; -P^0) = C\Gamma^{bT}_{PS}(-\vec{k}; -P^0)C^{-1}, \quad (3.19)$$

(T denotes the transpose). Taking the resonance Ansatz for Γ^{a5}_0, Eq. (3.11), or Γ^{a5}, Eq. (3.9) as appropriate, along with Eq. (3.18) for $G^{(4)}$, inserting into Eqs. (3.16) and (3.17), reorganizing the Dirac indices and evaluating the color and flavor traces, one obtains

$$r_{AV}P^0 \overset{P_0^2=M_{PS}^2}{=} -\iota N N_c \mathrm{Tr}_d \int đk \gamma^5 \gamma^0 W^+_{\bar{q}q}(k^+)\Gamma_{PS}(\vec{k}; P^0)$$
$$\times W^-_{\bar{q}q}(k^-),$$
$$r_{PS} \overset{P_0^2=M_{PS}^2}{=} \iota N N_c \mathrm{Tr}_d \int đk \gamma^5 W^+_{\bar{q}q}(k^+)\Gamma_{PS}(\vec{k}; P^0)$$
$$\times W^-_{\bar{q}q}(k^-). \quad (3.20)$$

The identity relating the residues, Eq. (3.13), can thus be written (independently of the normalization)

$$0 \overset{P_0^2=M_{PS}^2}{=} \mathrm{Tr}_d \int đk \gamma^5 [P^0\gamma^0 - (m^+ + m^-)]W^+_{\bar{q}q}(k^+)$$
$$\times \Gamma_{PS}(\vec{k}; P^0)W^-_{\bar{q}q}(k^-). \quad (3.21)$$

The leptonic decay constant for a pseudoscalar meson is defined as the coupling to the point axial field (see, for example, Refs. [26,34,35]). In Minkowski space and in the rest frame, it can be defined as (trace over Dirac matrices)

$$f_{PS} = \frac{N_c}{M_{PS}^2} \mathrm{Tr}_d \int đk \gamma^5 P^0 \gamma^0 W^+_{\bar{q}q}(k^+)\Gamma^N_{PS}(\vec{k}; P^0)W^-_{\bar{q}q}(k^-),$$
$$(3.22)$$

where Γ^N_{PS} is the normalized Bethe-Salpeter vertex function (the normalization will be discussed in the next section). It is useful to define a second quantity

$$h_{PS} = N_c \mathrm{Tr}_d \int đk \gamma^5 W^+_{\bar{q}q}(k^+)\Gamma^N_{PS}(\vec{k}; P^0)W^-_{\bar{q}q}(k^-), \quad (3.23)$$

such that Eq. (3.21) reads

$$M_{PS}^2 f_{PS} = (m^+ + m^-)h_{PS}. \quad (3.24)$$

In the chiral limit, the Gell-Mann-Oakes-Renner (GMOR) relation [35] states that

$$M_{PS}^2 f_{PS}^2 \overset{m^\pm \to 0}{=} -(m^+ + m^-)\langle \bar{q}q \rangle. \quad (3.25)$$

Comparing with Eq. (3.24), we see that in the chiral limit

$$h_{PS} \overset{m^\pm \to 0}{\to} -\frac{\langle \bar{q}q \rangle}{f_{PS}} = 2N_c \int đ\vec{k} \frac{M_k}{\omega_k f_{PS}}, \quad (3.26)$$

showing that h_{PS} is a generalization of the chiral condensate to finite quark masses. Comparison to the GMOR relation will define one method of normalizing Γ^N_{PS} aside from the canonical normalization (to be discussed later). Notice that with these conventions, one would have $f_\pi = 92.2$ MeV, a factor of $\sqrt{2}$ smaller than the convention used nowadays ($f_\pi = 130.4$ MeV as defined in Ref. [36]).

IV. PSEUDOSCALAR MESONS UNDER TRUNCATION

Having introduced the framework for studying the Bethe-Salpeter equation in Coulomb gauge and under the leading order truncation, let us now show how this framework can be applied. In this section, we shall be concerned with the pseudoscalar mesons; in the next section we shall repeat the analysis for vector mesons. Our aim is to show how the homogeneous Bethe-Salpeter equation for the meson mass, M_{PS}, the leptonic decay constant, f_{PS}, and the generalized condensate, h_{PS}, may be rewritten in terms of explicitly finite expressions despite the IR divergent interaction.

Removing the (overall) flavor factor, the general Dirac decomposition for the normalized pseudoscalar Bethe-Salpeter vertex, at resonance and in the rest frame, can be written

$$\Gamma^N_{PS}(\vec{p}; P^0) = \gamma^5[\Gamma^N_0(\vec{p}^2) + P^0\gamma^0\Gamma^N_1(\vec{p}^2) + \vec{\gamma} \cdot \vec{p}\Gamma^N_2(\vec{p}^2)$$
$$+ P^0\gamma^0\vec{\gamma} \cdot \vec{p}\Gamma^N_3(\vec{p}^2)]. \quad (4.1)$$

In principle, the scalar dressing functions Γ^N_i have the arguments $\Gamma^N_i(\vec{p}; P^0)$. However in practice, since the homogeneous Bethe-Salpeter equation used to derive these functions is valid only at resonance ($P_0^2 = M_{PS}^2$), the Γ^N_i are scalar functions of $\vec{p}^2$ alone and P^0 is merely a label. To condense the notation, we shall write the momentum dependence as a subscript, i.e., Γ^N_{ip}. Inserting the vertex decomposition, Eq. (4.1), into the expressions for f_{PS} and h_{PS}, Eqs. (3.22) and (3.23), respectively, expanding the quark propagators using Eq. (2.7), performing the Dirac traces and the energy integrals, one arrives at the following expressions:

$$f_{\mathrm{PS}} = 2\imath N_c \int \frac{d\vec{k}}{\omega_k^+ \omega_k^- [P_0^2 - (\tilde{\omega}_k^+ + \tilde{\omega}_k^-)^2]} \Big\{ \Gamma_{0k}^N [M_k^+ \omega_k^- + M_k^- \omega_k^+] + \Gamma_{2k}^N \vec{k}^2 [\omega_k^+ - \omega_k^-]$$
$$- (\tilde{\omega}_k^+ + \tilde{\omega}_k^-) \frac{[M_k^+ + M_k^-]}{[\omega_k^+ + \omega_k^-]} (\Gamma_{1k}^N [M_k^+ \omega_k^- + M_k^- \omega_k^+] + \Gamma_{3k}^N \vec{k}^2 [\omega_k^+ + \omega_k^-]) \Big\},$$

$$h_{\mathrm{PS}} = 2\imath N_c \int \frac{d\vec{k}}{\omega_k^+ \omega_k^- [P_0^2 - (\tilde{\omega}_k^+ + \tilde{\omega}_k^-)^2]} \Big\{ (\tilde{\omega}_k^+ + \tilde{\omega}_k^-) \frac{[\omega_k^+ + \omega_k^-]}{[M_k^+ + M_k^-]} (\Gamma_{0k}^N [M_k^+ \omega_k^- + M_k^- \omega_k^+]$$
$$+ \Gamma_{2k}^N \vec{k}^2 [\omega_k^+ - \omega_k^-]) - P_0^2 (\Gamma_{1k}^N [M_k^+ \omega_k^- + M_k^- \omega_k^+] + \Gamma_{3k}^N \vec{k}^2 [\omega_k^+ + \omega_k^-]) \Big\}, \tag{4.2}$$

where we have introduced the notation

$$\tilde{\omega}_k^{\pm} = A_k^{\pm} \omega_k^{\pm} \tag{4.3}$$

(in effect, the $\tilde{w}^{\pm}$ incorporate all the information about the IR divergence of the two quark self-energies and how they enter the expressions). We notice that in the above, the following common combinations of functions arise:

$$Q_{0k}^N = \Gamma_{0k}^N [M_k^+ \omega_k^- + M_k^- \omega_k^+] + \Gamma_{2k}^N \vec{k}^2 [\omega_k^+ - \omega_k^-], \qquad Q_{1k}^N = \Gamma_{1k}^N [M_k^+ \omega_k^- + M_k^- \omega_k^+] + \Gamma_{3k}^N \vec{k}^2 [\omega_k^+ + \omega_k^-], \tag{4.4}$$

allowing us to write

$$f_{\mathrm{PS}} = 2\imath N_c \int \frac{d\vec{k}}{\omega_k^+ \omega_k^- [P_0^2 - (\tilde{\omega}_k^+ + \tilde{\omega}_k^-)^2]} \Big\{ Q_{0k}^N - (\tilde{\omega}_k^+ + \tilde{\omega}_k^-) \frac{[M_k^+ + M_k^-]}{[\omega_k^+ + \omega_k^-]} Q_{1k}^N \Big\},$$
$$h_{\mathrm{PS}} = 2\imath N_c \int \frac{d\vec{k}}{\omega_k^+ \omega_k^- [P_0^2 - (\tilde{\omega}_k^+ + \tilde{\omega}_k^-)^2]} \Big\{ (\tilde{\omega}_k^+ + \tilde{\omega}_k^-) \frac{[\omega_k^+ + \omega_k^-]}{[M_k^+ + M_k^-]} Q_{0k}^N - P_0^2 Q_{1k}^N \Big\}. \tag{4.5}$$

As emphasized, one of the most important features of the above two quantities is that both are physical (h_{PS} reduces, up to constant prefactors, to the chiral condensate in the chiral limit) and, in particular, cannot contain unphysical IR divergences such as those contained within the functions $\tilde{\omega}^{\pm}$ (i.e., proportional to $A^{\pm}$). As mentioned previously, in the Coulomb gauge heavy quark limit it is known that the amputated connected four-point quark-antiquark Green's function, $G^{(4)}$, explicitly contains physical resonance poles [25]. However the residues of these poles contain IR divergent factors, meaning that via the decomposition Eq. (3.18), we can expect the Bethe-Salpeter vertex function Γ_{PS}^N and the components Γ_i^N to also involve IR divergent factors. This will be made explicit shortly. In anticipation of the cancellations necessary so that the expressions for f_{PS} and h_{PS} are indeed finite, let us define the dimensionless functions

$$f_k^N = \frac{1}{[P_0^2 - (\tilde{\omega}_k^+ + \tilde{\omega}_k^-)^2]} \Big\{ \frac{[\omega_k^+ + \omega_k^-]}{[M_k^+ + M_k^-]} Q_{0k}^N$$
$$- (\tilde{\omega}_k^+ + \tilde{\omega}_k^-) Q_{1k}^N \Big\},$$
$$h_k^N = \frac{1}{[P_0^2 - (\tilde{\omega}_k^+ + \tilde{\omega}_k^-)^2]} \Big\{ \frac{(\tilde{\omega}_k^+ + \tilde{\omega}_k^-)}{[M_k^+ + M_k^-]} Q_{0k}^N$$
$$- \frac{P_0^2}{[\omega_k^+ + \omega_k^-]} Q_{1k}^N \Big\}. \tag{4.6}$$

This gives the expressions

$$f_{\mathrm{PS}} = 2\imath N_c \int \frac{d\vec{k}}{\omega_k^+ \omega_k^-} \frac{[M_k^+ + M_k^-]}{[\omega_k^+ + \omega_k^-]} f_k^N, \tag{4.7}$$

$$h_{\mathrm{PS}} = 2\imath N_c \int \frac{d\vec{k}}{\omega_k^+ \omega_k^-} [\omega_k^+ + \omega_k^-] h_k^N. \tag{4.8}$$

Recall that in the chiral limit ($m^{\pm} \to 0$), Eq. (3.26) holds. Comparing with Eq. (4.8), we see that in terms of h_k^N this is equivalent to

$$h_k^N \overset{m^{\pm} \to 0}{\to} - \imath \frac{M_k}{2 f_{\mathrm{PS}}}. \tag{4.9}$$

Given that f_{PS} is a physical quantity and that the quark mass function, M, is IR finite, this limit tells us that indeed, h_k^N should also be IR finite. Further assuming a massless pion in the chiral limit and using the definitions Eqs. (4.4) and (4.6), h_k^N in the chiral limit can be written as

$$h_k^N \overset{m^{\pm} \to 0}{\to} - \frac{1}{4 \tilde{\omega}_k M_k} Q_{0k}^N = - \frac{1}{2 A_k} \Gamma_{0k}^N, \tag{4.10}$$

which would mean that the normalized Bethe-Salpeter vertex function component Γ_0^N obeys

$$\Gamma_{0k}^N \overset{m^{\pm} \to 0}{\to} \imath \frac{B_k}{f_{\mathrm{PS}}}. \tag{4.11}$$

This result agrees explicitly with the standard result (see, for example, Ref. [35]). Additionally, it confirms that the

Bethe-Salpeter vertex function and its components are IR divergent in exactly the same way as the quark self-energy.

Let us now turn to the homogeneous Bethe-Salpeter equation in the pseudoscalar channel, Eq. (3.10). Inserting the decompositions, Eq. (2.7) for the quark propagators and Eq. (4.1) for the pseudoscalar Bethe-Salpeter vertices, projecting out the Dirac components and performing the energy integrals one obtains four coupled homogeneous integral equations for the scalar functions Γ_i (un-normalized at this stage). However, careful inspection reveals that remarkably, all four equations have integrands involving precisely the combinations of factors used in the definitions of the functions f and h, Eqs. (4.4) and (4.6). The equations are:

$$\Gamma_{0p} = -\frac{1}{2}g^2 C_F \int \frac{d\vec{k}\,\tilde{F}(\vec{p}-\vec{k})}{\omega_k^+ \omega_k^-}[\omega_k^+ + \omega_k^-]h_k,$$

$$\Gamma_{1p} = \frac{1}{2}g^2 C_F \int \frac{d\vec{k}\,\tilde{F}(\vec{p}-\vec{k})}{\omega_k^+ \omega_k^-}\frac{[M_k^+ + M_k^-]}{[\omega_k^+ + \omega_k^-]}f_k,$$

$$\Gamma_{2p} = -\frac{1}{2}g^2 C_F \int \frac{d\vec{k}\,\tilde{F}(\vec{p}-\vec{k})}{\omega_k^+ \omega_k^-}\frac{\vec{p}\cdot\vec{k}}{\vec{p}^2}\frac{[M_k^+ \omega_k^- - M_k^- \omega_k^+]}{\vec{k}^2}h_k,$$

$$\Gamma_{3p} = \frac{1}{2}g^2 C_F \int \frac{d\vec{k}\,\tilde{F}(\vec{p}-\vec{k})}{\omega_k^+ \omega_k^-}\frac{\vec{p}\cdot\vec{k}}{\vec{p}^2}\frac{[M_k^+ + M_k^-]}{[M_k^+ \omega_k^- + M_k^- \omega_k^+]}f_k. \quad (4.12)$$

The structure of the above set of equations shows that, in general, the Bethe-Salpeter vertex with its four components is a convolution integral of the IR divergent

interaction, the quark mass functions (and associated quasiparticle energies) and the two putatively IR finite functions f and h. Notice that for equal quarks, Γ_2 vanishes. To arrive at a closed set of equations for f and h, we must invert their definitions in terms of the Γ_i. Using Eqs. (4.4) and (4.6), one may write

$$\frac{P_0^2}{[\omega_p^+ + \omega_p^-]^2}f_p - \frac{[\tilde{\omega}_p^+ + \tilde{\omega}_p^-]}{[\omega_p^+ + \omega_p^-]}h_p$$
$$= \Gamma_{0p}\frac{[M_p^+ \omega_p^- + M_p^- \omega_p^+]}{[\omega_p^+ + \omega_p^-][M_p^+ + M_p^-]} + \Gamma_{2p}\frac{\vec{p}^2[M_p^+ - M_p^-]}{[\omega_p^+ + \omega_p^-]^2},$$

$$\frac{[\tilde{\omega}_p^+ + \tilde{\omega}_p^-]}{[\omega_p^+ + \omega_p^-]}f_p - h_p$$
$$= \Gamma_{1p}\frac{[M_p^+ \omega_p^- + M_p^- \omega_p^+]}{[\omega_p^+ + \omega_p^-]} + \Gamma_{3p}\vec{p}^2. \quad (4.13)$$

Further, using the integral expression for the dressing function A, Eq. (2.11), one can rewrite the expression for $\tilde{\omega} = A\omega$ such that

$$\frac{[\tilde{\omega}_p^+ + \tilde{\omega}_p^-]}{[\omega_p^+ + \omega_p^-]} = 1 + \frac{1}{2}g^2 C_F \int \frac{d\vec{k}\,\tilde{F}(\vec{p}-\vec{k})}{\omega_k^+ \omega_k^-}\frac{\vec{p}\cdot\vec{k}}{\vec{p}^2}$$
$$\times \frac{[\omega_p^+ \omega_k^- + \omega_p^- \omega_k^+]}{[\omega_p^+ + \omega_p^-]}. \quad (4.14)$$

Substituting this integral expression and the integral forms for the Γ_i, Eq. (4.12), into Eq. (4.13) one finds the final coupled equations for f and h:

$$h_p = \frac{P_0^2}{[\omega_p^+ + \omega_p^-]^2}f_p + \frac{1}{2}g^2 C_F \int \frac{d\vec{k}\,\tilde{F}(\vec{p}-\vec{k})}{\omega_k^+ \omega_k^-}\left\{h_k\frac{[\omega_k^+ + \omega_k^-]}{[\omega_p^+ + \omega_p^-]}\left(\frac{[M_p^+ \omega_p^- + M_p^- \omega_p^+]}{[M_p^+ + M_p^-]} + \frac{\vec{p}\cdot\vec{k}}{\vec{k}^2}\frac{[M_k^+ \omega_k^- - M_k^- \omega_k^+][M_p^+ - M_p^-]}{[\omega_k^+ + \omega_k^-][\omega_p^+ + \omega_p^-]}\right)\right.$$
$$\left. - h_p\frac{\vec{p}\cdot\vec{k}}{\vec{p}^2}\frac{[\omega_p^+ \omega_k^- + \omega_p^- \omega_k^+]}{[\omega_p^+ + \omega_p^-]}\right\},$$

$$f_p = h_p + \frac{1}{2}g^2 C_F \int \frac{d\vec{k}\,\tilde{F}(\vec{p}-\vec{k})}{\omega_k^+ \omega_k^-}\left\{f_k\frac{[M_k^+ + M_k^-]}{[\omega_k^+ + \omega_k^-]}\left(\frac{[M_p^+ \omega_p^- + M_p^- \omega_p^+]}{[\omega_p^+ + \omega_p^-]} + \frac{\vec{p}\cdot\vec{k}[\omega_k^+ + \omega_k^-]}{[M_k^+ \omega_k^- + M_k^- \omega_k^+]}\right)\right.$$
$$\left. - f_p\frac{\vec{p}\cdot\vec{k}}{\vec{p}^2}\frac{[\omega_p^+ \omega_k^- + \omega_p^- \omega_k^+]}{[\omega_p^+ + \omega_p^-]}\right\}. \quad (4.15)$$

In both equations, the divergence (arising either from the δ-function charge constraint proportional to the divergent constant $\mathcal{C}$ or from the infrared singular $1/\vec{q}^4$ term in $\tilde{F}$) occurs when $\vec{p} = \vec{k}$. It is straightforward to show that in both cases, the remaining factors of the integrand cancel. Thus, the above integral equations are explicitly infrared finite and so are the functions f and h, as demanded by the definitions of f_{PS} and h_{PS}. Notice that if the meson were anything but a color-singlet, the cancellation of the divergences would not occur, just as in the case for the heavy quark limit [23–25]. Further, we see that the

only occurrence of $P_0^2 = M_{PS}^2$ lies in the coupling of f to the h-equation. That the system of four IR divergent components of the general pseudoscalar Bethe-Salpeter vertex decomposition reduces to a system of two finite functions is analogous to the case of the quark propagator, where the two IR divergent dressing functions (A and B) conspire to form the finite gap equation for the mass function, M.

In the special case where the quarks have equal mass, the above equations reduce significantly, although their general form remains the same. The equal mass equations read

$$h_p = \frac{P_0^2}{4\omega_p^2} f_p + \frac{1}{2} g^2 C_F \int \frac{d\vec{k}\, \tilde{F}(\vec{p} - \vec{k})}{\omega_k} \left\{ h_k - h_p \frac{\vec{p} \cdot \vec{k}}{\vec{p}^2} \right\},$$

$$f_p = h_p + \frac{1}{2} g^2 C_F \int \frac{d\vec{k}\, \tilde{F}(\vec{p} - \vec{k})}{\omega_k} \left\{ f_k \frac{[\vec{p} \cdot \vec{k} + M_p M_k]}{[\vec{k}^2 + M_k^2]} \right.$$

$$\left. - f_p \frac{\vec{p} \cdot \vec{k}}{\vec{p}^2} \right\}. \tag{4.16}$$

Comparing the first equation with the gap equation for the quark mass function, Eq. (2.13), one sees that the integral has the same form but with M replaced with h. Thus, it is clear that in the chiral limit, h is proportional to M (as shown in the discussion leading up to Eq. (4.9)) and $P_0^2 = M_{\mathrm{PS}}^2 = 0$, showing that the pion is massless in the chiral limit, as it should be.

It is worth pointing out a major difference between the Bethe-Salpeter equation above and studies performed within the covariant approach, e.g., Refs. [37–39]. In the covariant gauge approach, one works in Euclidean space and since the bound state total momentum is timelike, it is necessary to make an extension of the quark propagator to complex Euclidean momenta (usually numerically). This extension into the complex plane has the consequence that possible singularities must be treated carefully or avoided altogether (although numerical techniques to deal with such issues have been developed, e.g., Refs. [40–43]). For mesons of roughly equal quark masses this is not a major issue, however, for asymmetric systems such as heavy-light mesons this becomes challenging. In the Coulomb gauge rest frame (and Minkowski space) equations presented above, only the quark mass function (and quasiparticle energy) enters and is always evaluated at spatial momenta, rendering the issue of continuation to timelike momenta irrelevant (effectively, the energy integrals performed analytically in the derivation of the equations deal with this issue from the outset). It will be seen that heavy-light systems are no more difficult to treat than equal quark systems.

In order to calculate f_{PS} and h_{PS}, we must normalize the functions f and h. As a first derivation, let us consider the equal mass case where

$$f_{\mathrm{PS}} = 2\iota N_c \int \frac{d\vec{k}\, M_k}{\omega_k^3} f_k^N. \tag{4.17}$$

However, in the chiral limit, Eq. (4.9) holds such that we can write

$$M_k \overset{m \to 0}{\longrightarrow} 2\iota f_{\mathrm{PS}} h_k^N, \tag{4.18}$$

which would mean that the normalized functions must obey

$$1 \overset{m \to 0}{=} -4 N_c \int \frac{d\vec{k}}{\omega_k^3} f_k^N h_k^N, \tag{4.19}$$

in this limit, such that the GMOR relation, Eq. (3.25), is satisfied. We see that in this restricted limit, the normalization can be written in terms of our finite functions f and h. More properly, the canonical normalization of the Bethe-Salpeter vertex function reads (in the Minkowski space rest frame and with trace over color, flavor and Dirac matrices) [35]

$$2\iota \delta^{ab} P^0 = \mathrm{Tr}_{f,c,d} \int d\!\!{}^- k \left\{ \bar{\Gamma}_{\mathrm{PS}}^{aN}(\vec{k}; -P^0) \frac{\partial W_{\bar{q}q}^+(k^+)}{\partial P^0} \right.$$

$$\times \Gamma_{\mathrm{PS}}^{bN}(\vec{k}; P^0) W_{\bar{q}q}^-(k^-)$$

$$\left. + \bar{\Gamma}_{\mathrm{PS}}^{aN}(\vec{k}; -P^0) W_{\bar{q}q}^+(k^+) \Gamma_{\mathrm{PS}}^{bN}(\vec{k}; P^0) \frac{\partial W_{\bar{q}q}^-(k^-)}{\partial P^0} \right\}. \tag{4.20}$$

Evaluating the flavor (recall that we have $N_f = 2$ and consider flavor nonsinglet mesons) and color traces, and using

$$\frac{\partial W_{\bar{q}q}^\pm(k^\pm)}{\partial P^0} = -W_{\bar{q}q}^\pm(k^\pm) \frac{\partial \Gamma_{\bar{q}q}^\pm(k^\pm)}{\partial P^0} W_{\bar{q}q}^\pm(k^\pm),$$

$$\frac{\partial \Gamma_{\bar{q}q}^\pm(k^\pm)}{\partial P^0} = \pm \frac{\iota}{2} \gamma^0, \tag{4.21}$$

one obtains

$$1 = -\frac{N_c}{2P^0} \mathrm{Tr}_d \int d\!\!{}^- k \bar{\Gamma}_{\mathrm{PS}}^N(\vec{k}; -P^0) W_{\bar{q}q}^+(k^+) \{ \gamma^0 W_{\bar{q}q}^+(k^+)$$

$$\times \Gamma_{\mathrm{PS}}^N(\vec{k}; P^0) - \Gamma_{\mathrm{PS}}^N(\vec{k}; P^0) W_{\bar{q}q}^-(k^-) \gamma^0 \} W_{\bar{q}q}^-(k^-). \tag{4.22}$$

The (Dirac structure of the) conjugate Bethe-Salpeter vertex function is explicitly given in the rest frame by

$$\bar{\Gamma}^N(\vec{k}; -P^0) = C \Gamma^{\mathrm{NT}}(-\vec{k}; -P^0) C^{-1}$$

$$= \gamma^5 [\Gamma_{0k}^N - P^0 \gamma^0 \Gamma_{1k}^N - \vec{\gamma} \cdot \vec{k} \Gamma_{2k}^N - P^0 \gamma^0 \vec{\gamma} \cdot \vec{k} \Gamma_{3k}^N]. \tag{4.23}$$

After evaluating the Dirac trace and performing the energy integrals, one finds after some effort that the normalization condition can be written in terms of the finite functions f and h:

$$1 = -4 N_c \int \frac{d\vec{k}\, f_k^N h_k^N}{\omega_k^+ \omega_k^-} \frac{[M_k^+ + M_k^-]}{[M_k^+ \omega_k^- + M_k^- \omega_k^+]}, \tag{4.24}$$

which reduces explicitly for equal mass quarks to the earlier form Eq. (4.19). Given an arbitrarily normalized solution to the Bethe-Salpeter equation, Eq. (4.15), (we shall use the condition $h(\vec{p}^2 \to 0) = 1$ for the numerical analysis later on) it is useful to write

$$f_k^N = \frac{f_k}{\iota \mathcal{N}}, \qquad h_k^N = \frac{h_k}{\iota \mathcal{N}}. \tag{4.25}$$

This then results in the normalization condition

$$\mathcal{N}^2 = 4N_c \int \frac{d\vec{k} f_k h_k}{\omega_k^+ \omega_k^-} \frac{[M_k^+ + M_k^-]}{[M_k^+ \omega_k^- + M_k^- \omega_k^+]} \qquad (4.26)$$

and the redefinition of f_{PS} and h_{PS} to

$$f_{\mathrm{PS}} = \frac{2N_c}{\mathcal{N}} \int \frac{d\vec{k}}{\omega_k^+ \omega_k^-} \frac{[M_k^+ + M_k^-]}{[\omega_k^+ + \omega_k^-]} f_k, \qquad (4.27)$$

$$h_{\mathrm{PS}} = \frac{2N_c}{\mathcal{N}} \int \frac{d\vec{k}}{\omega_k^+ \omega_k^-} [\omega_k^+ + \omega_k^-] h_k. \qquad (4.28)$$

Recall that it is known that the Coulomb gauge quark propagator under this truncation reduces to its heavy quark limit (in the absence of pure Yang-Mills theory corrections) [30]. The difference between the mass function and the bare mass becomes smaller in the heavy quark limit, i.e., $M_k - m_h \to 0$ as $m_h \to \infty$ (we will use m_h to denote the heavy quark mass). For a heavy-light system, with $m^+ = m_h \to \infty$ and assuming that the above integrals for $\mathcal{N}$, f_{PS} and h_{PS} converge for large $\vec{k}$ (i.e., that the convergence is driven by the large $\vec{k}$ behavior of the functions f_k and h_k) then we can make the replacement $\omega_k^+ = M_k^+ = m_h \gg \omega_k^-, M_k^-$ within the integrals. This then gives

$$\mathcal{N}^2 \overset{m^+=m_h}{\to} \frac{4N_c}{m_h} \int \frac{d\vec{k} f_k h_k}{\omega_k^- [\omega_k^- + M_k^-]},$$

$$f_{\mathrm{PS}} \overset{m^+=m_h}{\to} \frac{2N_c}{\mathcal{N} m_h} \int \frac{d\vec{k}}{\omega_k^-} f_k, \qquad (4.29)$$

$$h_{\mathrm{PS}} \overset{m^+=m_h}{\to} \frac{2N_c}{\mathcal{N}} \int \frac{d\vec{k}}{\omega_k^-} h_k.$$

Performing the same substitution for Eq. (4.15) gives

$$h_p \overset{m^+=m_h}{\to} \frac{P_0^2}{m_h^2} f_p + \mathcal{O}(1/m_h),$$

$$f_p \overset{m^+=m_h}{\to} h_p + \mathcal{O}(1/m_h), \qquad (4.30)$$

which tells us that (asymptotically, as $m_h \to \infty$) $P_0^2 = M_{\mathrm{PS}}^2 = m_h^2$ as we would expect. We notice though, that the leading order heavy quark limit merely tells us that $f_p = h_p$, but not what f_p or h_p actually are. With the above limits for M_{PS}, f_{PS} and h_{PS}, we see that the relationship Eq. (3.24) is explicitly fulfilled. The most important result of this analysis though, is that as $m_h \to \infty$ (assuming the integrals are well-defined) and given $\mathcal{N} \sim 1/\sqrt{m_h}$,

$$f_{\mathrm{PS}} \sqrt{M_{\mathrm{PS}}} \sim \text{const.} \qquad (4.31)$$

This result explicitly agrees with the analysis of heavy quark effective theory at leading order [44].

At this stage, it is appropriate to make a comparison of the formalism presented here with similar works on the Coulomb gauge Bethe-Salpeter equation. As mentioned earlier, the chiral limit pseudoscalar meson (i.e., the

pion) was investigated in Ref. [26]. An extension to the case of equal, but finite mass quarks was performed in, e.g., Refs. [28,45,46]. The equations therein have subtle differences to those presented here, over and above the obvious extension to arbitrary quark masses. Since the referenced works dealt with equal mass quarks, the vertex component Γ_2 was absent from the outset although they explicitly found that the system can be decomposed in terms of two finite functions. The coupled equations for the two finite functions (f and h) presented here are, from the point of view of canceling the IR divergences, somewhat more explicit than the earlier versions since the IR divergent factors ($\tilde{\omega}$ in our notation) inherent to the quark self-energy have been completely eliminated. This elimination also extends to the equations for f_{PS}, h_{PS} and the normalization. The success of making this cancellation explicit arises from utilizing a different definition of the two functions, Eq. (4.6), designed with the arbitrary quark mass expressions for f_{PS} and h_{PS} in mind. This is in distinction to the original decomposition of Refs. [26,28], whose motivation was to make the Bethe-Salpeter equation tractable. Despite the differences in the decomposition, both sets of functions yield finite quantities.

V. VECTOR MESONS UNDER TRUNCATION

Let us now consider vector mesons. Although the expressions are considerably more involved than those discussed in the previous section, they follow the same pattern. The homogeneous Bethe-Salpeter equation retains its form as for the pseudoscalar case, Eq. (3.10),

$$\Gamma_{Vi}^a(\vec{p}; P^0) \overset{P_0^2=M_V^2}{=} -\imath g^2 C_F \int d k \tilde{F}(\vec{p} - \vec{k}) \gamma^0 W_{\bar{q}q}^+(k^+)$$
$$\times \Gamma_{Vi}^a(\vec{k}; P^0) W_{\bar{q}q}^-(k^-) \gamma^0, \qquad (5.1)$$

but the general decomposition of the normalized vector Bethe-Salpeter vertex function (in the rest frame and omitting the flavor dependence) now reads

$$\Gamma_{Vi}^N(\vec{p}; P^0) = \{ \gamma^i [\Gamma_{0p}^N + P^0 \gamma^0 \Gamma_{1p}^N + \vec{\gamma} \cdot \vec{p} \Gamma_{2p}^N + P^0 \gamma^0 \vec{\gamma} \cdot \vec{p} \Gamma_3^N]$$
$$+ p^i [\Gamma_{2p}^N + \Gamma_{4p}^N + P^0 \gamma^0 (\Gamma_{5p}^N - \Gamma_{3p}^N) + \vec{\gamma} \cdot \vec{p} \Gamma_{6p}^N$$
$$+ P^0 \gamma^0 \vec{\gamma} \cdot \vec{p} \Gamma_{7p}^N] \}, \qquad (5.2)$$

where it is recognized that the vector meson at resonance is transverse to the total four-momentum P and so, can only have spatial components. The vector meson leptonic decay constant can be defined as (trace over Dirac matrices) [38]

$$f_V = -\frac{N_c}{3 M_V} \mathrm{Tr}_d \int d k \gamma^i W_{\bar{q}q}^+(k^+) \Gamma_{Vi}^N(\vec{k}; P^0) W_{\bar{q}q}^-(k^-), \quad (5.3)$$

and the normalization defined as (trace over color, flavor and Dirac matrices)

$$6\iota\delta^{ab}P^0 = \mathrm{Tr}_{f,c,d}\int d\!\!\!/k\left\{\bar\Gamma_{Vi}^{aN}(\vec k;-P^0)\frac{\partial W_{\bar qq}^+(k^+)}{\partial P^0}\Gamma_{Vi}^{bN}(\vec k;P^0)W_{\bar qq}^-(k^-)+\bar\Gamma_{Vi}^{aN}(\vec k;-P^0)W_{\bar qq}^+(k^+)\Gamma_{Vi}^{bN}(\vec k;P^0)\frac{\partial W_{\bar qq}^-(k^-)}{\partial P^0}\right\}. \quad (5.4)$$

In both the latter equations, a factor of three arises from the (transverse) polarization states of the vector meson. With the definition of the conjugate amplitude as before:

$$\bar\Gamma_{Vi}^N(\vec k;-P^0)=C\Gamma_{Vi}^{NT}(-\vec k;-P^0)C^{-1}, \quad (5.5)$$

one has

$$\bar\Gamma_{Vi}^N(\vec k;-P^0)=\gamma^i[-\Gamma_{0k}^N+P^0\gamma^0\Gamma_{1k}^N+\vec\gamma\cdot\vec k\Gamma_{2k}^N+P^0\gamma^0\vec\gamma\cdot\vec k\Gamma_{3k}^N]+k^i[\Gamma_{2k}^N-\Gamma_{4k}^N-P^0\gamma^0(\Gamma_{5k}^N+\Gamma_{3k}^N)$$
$$-\vec\gamma\cdot\vec k\Gamma_{6k}^N+P^0\gamma^0\vec\gamma\cdot\vec k\Gamma_{7k}^N]. \quad (5.6)$$

Starting with the leptonic decay constant, f_V, defined in Eq. (5.3), after inserting the decompositions for the Bethe-Salpeter vertex, Eq. (5.2), and the quark propagator, Eq. (2.7), evaluating the trace over Dirac matrices and performing the energy integrals, one has the expression

$$f_V=-\frac{2\iota N_c}{3M_V}\int\frac{d\!\!\!/\vec k}{\omega_k^+\omega_k^-[P_0^2-(\tilde\omega_k^++\tilde\omega_k^-)^2]}\left\{(\tilde\omega_k^++\tilde\omega_k^-)\left[-2\frac{[\omega_k^++\omega_k^-]}{[M_k^++M_k^-]}(\Gamma_{0k}^N[M_k^+\omega_k^-+M_k^-\omega_k^+]+\Gamma_{2k}^N\vec k^2[\omega_k^+-\omega_k^-])\right.\right.$$
$$-\frac{[M_k^++M_k^-]}{[\omega_k^++\omega_k^-]}([\Gamma_{0k}^N+\vec k^2\Gamma_{6k}^N][M_k^+\omega_k^-+M_k^-\omega_k^+]-\Gamma_{4k}^N\vec k^2[\omega_k^++\omega_k^-])\bigg]+P_0^2[2\Gamma_{1k}^N[M_k^+\omega_k^-+M_k^-\omega_k^+]$$
$$+2\Gamma_{3k}^N\vec k^2[\omega_k^++\omega_k^-]+[\Gamma_{1k}^N-\vec k^2\Gamma_{7k}^N][M_k^+\omega_k^-+M_k^-\omega_k^+]+\Gamma_{5k}^N\vec k^2[\omega_k^+-\omega_k^-]]\bigg\}. \quad (5.7)$$

Interestingly, we note the appearance of the combinations of functions Q_0^N and Q_1^N, Eq. (4.4), defined for the pseudoscalar meson. Introducing the further two combinations

$$Q_{2k}^N=[\Gamma_{0k}^N+\vec k^2\Gamma_{6k}^N][M_k^+\omega_k^-+M_k^-\omega_k^+]-\Gamma_{4k}^N\vec k^2[\omega_k^++\omega_k^-],$$
$$Q_{3k}^N=[\Gamma_{1k}^N-\vec k^2\Gamma_{7k}^N][M_k^+\omega_k^-+M_k^-\omega_k^+]+\Gamma_{5k}^N\vec k^2[\omega_k^+-\omega_k^-], \quad (5.8)$$

we can write

$$f_V=\frac{2\iota N_c}{3M_V}\int\frac{d\!\!\!/\vec k}{\omega_k^+\omega_k^-[P_0^2-(\tilde\omega_k^++\tilde\omega_k^-)^2]}\left\{(\tilde\omega_k^++\tilde\omega_k^-)\left[2\frac{[\omega_k^++\omega_k^-]}{[M_k^++M_k^-]}Q_{0k}^N+\frac{[M_k^++M_k^-]}{[\omega_k^++\omega_k^-]}Q_{2k}^N\right]-P_0^2[2Q_{1k}^N+Q_{3k}^N]\right\}. \quad (5.9)$$

We identify the appearance of h_k^N (defined in Eq. (4.6) for the pseudoscalar meson) in this equation and introduce, in analogy to before, the dimensionless functions

$$g_k^N=\frac{1}{[P_0^2-(\tilde\omega_k^++\tilde\omega_k^-)^2]}\left\{Q_{2k}^N-\frac{(\tilde\omega_k^++\tilde\omega_k^-)[\omega_k^++\omega_k^-]}{[M_k^++M_k^-]}Q_{3k}^N\right\},$$
$$j_k^N=\frac{1}{[P_0^2-(\tilde\omega_k^++\tilde\omega_k^-)^2]}\left\{\frac{(\tilde\omega_k^++\tilde\omega_k^-)}{[\omega_k^++\omega_k^-]}Q_{2k}^N-\frac{P_0^2}{[M_k^++M_k^-]}Q_{3k}^N\right\}, \quad (5.10)$$

where the function g_k^N will shortly be needed and the aim will be to see if these functions are finite. The vector meson leptonic decay constant can thus be written as

$$f_V=\frac{2\iota N_c}{3M_V}\int\frac{d\!\!\!/\vec k}{\omega_k^+\omega_k^-}(2[\omega_k^++\omega_k^-]h_k^N+[M_k^++M_k^-]j_k^N). \quad (5.11)$$

The above expression has an almost identical form as for the pseudoscalar case, Eq. (4.7).

Turning now to the vector meson Bethe-Salpeter equation, Eq. (5.1), after inserting the decompositions for the Bethe-Salpeter vertex, Eq. (5.2), and quark propagator, Eq. (2.7), projecting out the Dirac structure and performing the energy integrals, one can identify the appearance of precisely the combinations of

(unnormalized) functions that define f_k, h_k, g_k and j_k, Eqs. (4.6) and (5.10), (the former two defined for the pseudoscalar meson) in exactly the same way as previously. That there are only four combinations means that there are only four independent dynamical functions that characterize the vector meson under this truncation. The equations for the vector meson Γ_i read:

$$\Gamma_{0p} = \frac{1}{2} g^2 C_F \int \frac{d\vec{k}\, \tilde{F}(\vec{p} - \vec{k})}{\omega_k^+ \omega_k^-} \left\{ \left(\frac{\Delta}{2} - 1\right)[\omega_k^+ + \omega_k^-] h_k - \frac{\Delta}{2}[M_k^+ + M_k^-] j_k \right\},$$

$$\Gamma_{1p} = \frac{1}{2} g^2 C_F \int \frac{d\vec{k}\, \tilde{F}(\vec{p} - \vec{k})}{\omega_k^+ \omega_k^-} \left\{ \left(1 - \frac{\Delta}{2}\right) \frac{[M_k^+ + M_k^-]}{[\omega_k^+ + \omega_k^-]} f_k + \frac{\Delta}{2} g_k \right\},$$

$$\Gamma_{2p} = \frac{1}{2} g^2 C_F \int \frac{d\vec{k}\, \tilde{F}(\vec{p} - \vec{k})}{\omega_k^+ \omega_k^-} \frac{\vec{p} \cdot \vec{k}}{\vec{p}^2 \vec{k}^2} [M_k^+ \omega_k^- - M_k^- \omega_k^+][-h_k],$$

$$\Gamma_{3p} = \frac{1}{2} g^2 C_F \int \frac{d\vec{k}\, \tilde{F}(\vec{p} - \vec{k})}{\omega_k^+ \omega_k^-} \frac{\vec{p} \cdot \vec{k}}{\vec{p}^2} \frac{[M_k^+ + M_k^-]}{[M_k^+ \omega_k^- + M_k^- \omega_k^+]} f_k,$$

$$\Gamma_{4p} = \frac{1}{2} g^2 C_F \int \frac{d\vec{k}\, \tilde{F}(\vec{p} - \vec{k})}{\omega_k^+ \omega_k^-} \frac{\vec{p} \cdot \vec{k}}{\vec{p}^2} \frac{[\omega_k^+ + \omega_k^-][M_k^+ + M_k^-]}{[M_k^+ \omega_k^- + M_k^- \omega_k^+]} j_k,$$

$$\Gamma_{5p} = \frac{1}{2} g^2 C_F \int \frac{d\vec{k}\, \tilde{F}(\vec{p} - \vec{k})}{\omega_k^+ \omega_k^-} \frac{\vec{p} \cdot \vec{k}}{\vec{p}^2} \frac{[\omega_k^+ - \omega_k^-]}{[M_k^+ \omega_k^- + M_k^- \omega_k^+]} g_k,$$

$$\Gamma_{6p} = \frac{1}{2} g^2 C_F \int \frac{d\vec{k}\, \tilde{F}(\vec{p} - \vec{k})}{\omega_k^+ \omega_k^-} \frac{1}{\vec{p}^2} \left(1 - \frac{3\Delta}{2}\right) \{[\omega_k^+ + \omega_k^-] h_k - [M_k^+ + M_k^-] j_k\},$$

$$\Gamma_{7p} = \frac{1}{2} g^2 C_F \int \frac{d\vec{k}\, \tilde{F}(\vec{p} - \vec{k})}{\omega_k^+ \omega_k^-} \frac{1}{\vec{p}^2} \left(1 - \frac{3\Delta}{2}\right) \left\{ \frac{[M_k^+ + M_k^-]}{[\omega_k^+ + \omega_k^-]} f_k - g_k \right\},$$

$$(5.12)$$

where we write

$$\Delta = 1 - \frac{\vec{p} \cdot \vec{k}^2}{\vec{p}^2 \vec{k}^2}. \tag{5.13}$$

Assuming that the functions f_k, h_k, g_k and j_k are finite (as we shall shortly demonstrate), the vector meson Bethe-Salpeter vertex Γ_V (and its components, Γ_i) is given as a

convolution integral involving the IR divergent interaction and the quark mass functions, just as for the pseudoscalar meson. Further, we notice that if we artificially set $\Delta = 0$, the first four equations are identical to those in the pseudoscalar case. In the special case of equal mass quarks, Γ_2 and Γ_5 vanish. Inverting the definitions of g_k and j_k, Eq. (5.10), one has

$$P_0^2 g_p - [\tilde{\omega}_p^+ + \tilde{\omega}_p^-][\omega_p^+ + \omega_p^-] j_p = (\Gamma_{0p} + \vec{p}^2 \Gamma_{6p})[M_p^+ \omega_p^- + M_p^- \omega_p^+] - \Gamma_{4p} \vec{p}^2 [\omega_p^+ + \omega_p^-],$$

$$\frac{[\tilde{\omega}_p^+ + \tilde{\omega}_p^-]}{[\omega_p^+ + \omega_p^-]} g_p - j_p = (\Gamma_{1p} - \vec{p}^2 \Gamma_{7p}) \frac{[M_p^+ \omega_p^- + M_p^- \omega_p^+]}{[M_p^+ + M_p^-]} + \Gamma_{5p} \vec{p}^2 \frac{[\omega_p^+ - \omega_p^-]}{[M_p^+ + M_p^-]},$$

$$(5.14)$$

in addition to the analogous expressions defined as for the pseudoscalar case, Eq. (4.13). Collecting together the definitions, along with Eq. (4.14) for the factors involving $\tilde{\omega}$, this results in the following four equations:

$$
h_p = \frac{P_0^2}{[\omega_p^+ + \omega_p^-]^2} f_p + \frac{1}{2} g^2 C_F \int \frac{d\vec{k}\, \tilde{F}(\vec{p} - \vec{k})}{\omega_k^+ \omega_k^-} \left\{ \left[\left(1 - \frac{\Delta}{2} \right) [\omega_k^+ + \omega_k^-] h_k + \frac{\Delta}{2} [M_k^+ + M_k^-] j_k \right] \frac{[M_p^+ \omega_p^- + M_p^- \omega_p^+]}{[\omega_p^+ + \omega_p^-][M_p^+ + M_p^-]} \right.
$$
$$
\left. + h_k \frac{\vec{p} \cdot \vec{k}}{\vec{k}^2} \frac{[M_k^+ \omega_k^- - M_k^- \omega_k^+][M_p^+ - M_p^-]}{[\omega_p^+ + \omega_p^-]^2} - h_p \frac{\vec{p} \cdot \vec{k}}{\vec{p}^2} \frac{[\omega_p^+ \omega_k^- + \omega_p^- \omega_k^+]}{[\omega_p^+ + \omega_p^-]} \right\},
$$

$$
f_p = h_p + \frac{1}{2} g^2 C_F \int \frac{d\vec{k}\, \tilde{F}(\vec{p} - \vec{k})}{\omega_k^+ \omega_k^-} \left\{ \left[\left(1 - \frac{\Delta}{2} \right) \frac{[M_k^+ + M_k^-]}{[\omega_k^+ + \omega_k^-]} f_k + \frac{\Delta}{2} g_k \right] \frac{[M_p^+ \omega_p^- + M_p^- \omega_p^+]}{[\omega_p^+ + \omega_p^-]} + f_k \frac{\vec{p} \cdot \vec{k}[M_k^+ + M_k^-]}{[M_k^+ \omega_k^- + M_k^- \omega_k^+]} \right.
$$
$$
\left. - f_p \frac{\vec{p} \cdot \vec{k}}{\vec{p}^2} \frac{[\omega_p^+ \omega_k^- + \omega_p^- \omega_k^+]}{[\omega_p^+ + \omega_p^-]} \right\},
$$

$$
j_p = \frac{P_0^2}{[\omega_p^+ + \omega_p^-]^2} g_p + \frac{1}{2} g^2 C_F \int \frac{d\vec{k}\, \tilde{F}(\vec{p} - \vec{k})}{\omega_k^+ \omega_k^-} \left\{ \left[\frac{\vec{p} \cdot \vec{k}^2}{\vec{p}^2 \vec{k}^2} [M_k^+ + M_k^-] j_k + \Delta [\omega_k^+ + \omega_k^-] h_k \right] \frac{[M_p^+ \omega_p^- + M_p^- \omega_p^+]}{[\omega_p^+ + \omega_p^-]^2} \right.
$$
$$
\left. + j_k \frac{\vec{p} \cdot \vec{k}[\omega_k^+ + \omega_k^-][M_k^+ + M_k^-]}{[\omega_p^+ + \omega_p^-][M_k^+ \omega_k^- + M_k^- \omega_k^+]} - j_p \frac{\vec{p} \cdot \vec{k}}{\vec{p}^2} \frac{[\omega_p^+ \omega_k^- + \omega_p^- \omega_k^+]}{[\omega_p^+ + \omega_p^-]} \right\},
$$

$$
g_p = j_p + \frac{1}{2} g^2 C_F \int \frac{d\vec{k}\, \tilde{F}(\vec{p} - \vec{k})}{\omega_k^+ \omega_k^-} \left\{ \left[\frac{\vec{p} \cdot \vec{k}^2}{\vec{p}^2 \vec{k}^2} g_k + \Delta \frac{[M_k^+ + M_k^-]}{[\omega_k^+ + \omega_k^-]} f_k \right] \frac{[M_p^+ \omega_p^- + M_p^- \omega_p^+]}{[M_p^+ + M_p^-]} \right.
$$
$$
\left. + g_k \frac{\vec{p} \cdot \vec{k}[\omega_k^+ - \omega_k^-][\omega_p^+ - \omega_p^-]}{[M_k^+ \omega_k^- + M_k^- \omega_k^+][M_p^+ + M_p^-]} - g_p \frac{\vec{p} \cdot \vec{k}}{\vec{p}^2} \frac{[\omega_p^+ \omega_k^- + \omega_p^- \omega_k^+]}{[\omega_p^+ + \omega_p^-]} \right\}. \tag{5.15}
$$

As before for the pseudoscalar mesons, the singularities arising from $\tilde{F}$ when $\vec{p} = \vec{k}$ cancel, showing that all four functions are indeed finite. In the equal mass case, the equations reduce to

$$
h_p = \frac{P_0^2}{4\omega_p^2} f_p + \frac{1}{2} g^2 C_F \int \frac{d\vec{k}\, \tilde{F}(\vec{p} - \vec{k})}{\omega_k} \left\{ \left(1 - \frac{\Delta}{2} \right) h_k - h_p \frac{\vec{p} \cdot \vec{k}}{\vec{p}^2} + \frac{\Delta}{2} \frac{M_k}{\omega_k} j_k \right\},
$$
$$
f_p = h_p + \frac{1}{2} g^2 C_F \int \frac{d\vec{k}\, \tilde{F}(\vec{p} - \vec{k})}{\omega_k} \left\{ \left(1 - \frac{\Delta}{2} \right) \frac{M_p M_k}{\omega_k^2} f_k + \frac{\vec{p} \cdot \vec{k}}{\omega_k^2} f_k - f_p \frac{\vec{p} \cdot \vec{k}}{\vec{p}^2} + \frac{\Delta}{2} \frac{M_p}{\omega_k} g_k \right\},
$$
$$
j_p = \frac{P_0^2}{4\omega_p^2} g_p + \frac{1}{2} g^2 C_F \int \frac{d\vec{k}\, \tilde{F}(\vec{p} - \vec{k})}{\omega_k} \left\{ \frac{\vec{p} \cdot \vec{k}^2}{\vec{p}^2 \vec{k}^2} \frac{M_p M_k}{\omega_p \omega_k} j_k + \frac{\vec{p} \cdot \vec{k}}{\omega_p \omega_k} j_k - j_p \frac{\vec{p} \cdot \vec{k}}{\vec{p}^2} + \Delta \frac{M_p}{\omega_p} h_k \right\},
$$
$$
g_p = j_p + \frac{1}{2} g^2 C_F \int \frac{d\vec{k}\, \tilde{F}(\vec{p} - \vec{k})}{\omega_k} \left\{ \frac{\vec{p} \cdot \vec{k}^2}{\vec{p}^2 \vec{k}^2} \frac{\omega_p}{\omega_k} g_k - g_p \frac{\vec{p} \cdot \vec{k}}{\vec{p}^2} + \Delta \frac{\omega_p M_k}{\omega_k^2} f_k \right\}. \tag{5.16}
$$

The above sets of coupled equations have a rather illuminating structure. One sees that outside the integrals, the functions (f, h) and (g, j) appear pairwise, each with only one occurrence of $P_0^2 = M_V^2$. Inside the integral, the pairing is (f, g) and (h, j). This pairwise connection will be visible in the numerical solutions. Within the integrals, the pairing comes with an associated factor of Δ that serves to couple the two sets of equations for the pairings (f, h) and (g, j) (hence the decoupling when Δ is artificially set to zero). Δ, as defined in Eq. (5.13), is dependent only on the angle between the spatial momenta $\vec{p}$ and $\vec{k}$. That when an angular dependence is suppressed, the equations for the vector meson reduce to those of the pseudoscalar has an obvious interpretation: the emergence of the quantum mechanical description of the vector meson as being a total angular momentum excitation of the groundstate (pseudoscalar) meson, even in the context of the relativistic (though noncovariant) Bethe-Salpeter framework used here.

The normalization of the vector meson Bethe-Salpeter vertex function can now be discussed. Taking Eq. (5.4), inserting the vector meson vertex decomposition, Eq. (5.2), its conjugate, Eq. (5.6), along with Eq. (2.7) for the quark propagator and treating as for the pseudoscalar case, the result is

$$
1 = -\frac{4N_c}{3} \int \frac{d\vec{k}}{\omega_k^+ \omega_k^-} [2 f_k^N h_k^N + g_k^N j_k^N] \frac{[M_k^+ + M_k^-]}{[M_k^+ \omega_k^- + M_k^- \omega_k^+]}, \tag{5.17}
$$

or, for equal mass quarks

$$1 = -\frac{4N_c}{3} \int \frac{d\vec{k}}{\omega_k^3} [2f_k^N h_k^N + g_k^N j_k^N], \tag{5.18}$$

and where again, only the finite combinations f_k, h_k, g_k and j_k defined in Eqs. (4.6) and (5.10) appear. Just as for the leptonic decay constants and the Bethe-Salpeter equations, the vector meson normalization has the same structure as for the pseudoscalar case, Eq. (4.24).

Finally, let us discuss the heavy quark limit for the vector meson. This proceeds as for the pseudoscalar case. With the normalization convention that

$$g_p^N = \frac{g_p}{\iota \mathcal{N}}, \qquad j_p^N = \frac{j_p}{\iota \mathcal{N}} \tag{5.19}$$

(h_p and f_p as in Eq. (4.25) and with $h(\vec{p}^2 \rightarrow 0) = 1$), we have from the normalization that ($m^+ = m_h \rightarrow \infty$ as before)

$$\mathcal{N}^2 \overset{m^+ = m_h}{\rightarrow} \frac{4N_c}{3m_h} \int \frac{d\vec{k}}{\omega_k^- [\omega_k^- + M_k^-]} [2f_k h_k + g_k j_k], \tag{5.20}$$

or $\mathcal{N} \sim 1/\sqrt{m_h}$. The vector meson leptonic decay constant, Eq. (5.11), becomes

$$f_V \overset{m^+ = m_h}{\rightarrow} \frac{2N_c}{3\mathcal{N} M_V} \int \frac{d\vec{k}}{\omega_k} (2h_k + j_k). \tag{5.21}$$

The vector meson Bethe-Salpeter equation, Eq. (5.15), gives us the further information that $f_p = h_p$, $j_p = g_p$ and $M_V = m_h$ in the heavy quark limit, such that as $m_h \rightarrow \infty$,

$$f_V \sqrt{M_V} \sim \text{const.} \tag{5.22}$$

Again, this agrees with the known heavy quark limit at leading order [44]. There is one further result that we should check and this concerns the ratio f_V/f_{PS}. The heavy quark effective theory result at leading order is [44]

$$\frac{f_V}{f_{\text{PS}}} = 1 - \frac{2\alpha_s(m_h)}{3\pi} \tag{5.23}$$

(α_s being evaluated at the scale m_h). In our case, we do not include α_s contributions, so we should see that for heavy-light systems as $m^+ = m_h \rightarrow \infty$

$$\frac{f_V}{f_{\text{PS}}} \overset{m^+ = m_h}{\rightarrow} 1. \tag{5.24}$$

VI. NUMERICAL IMPLEMENTATION

Before presenting the results, it is worthwhile discussing the numerical implementation of the equations. While the infrared singularities of the interaction do cancel formally, they present a formidable challenge for the numerical analysis. The techniques used are based on those employed to solve the gap equation for the quark mass function M_k, Eq. (2.13), explained in detail in Ref. [30].

As a concrete example, let us consider the equal quark mass pseudoscalar meson Bethe-Salpeter equation for h_p, Eq. (4.16), which reads

$$h_p = \frac{P_0^2}{4\omega_p^2} f_p + \frac{1}{2} g^2 C_F \int \frac{d\vec{k}\, \tilde{F}(\vec{p} - \vec{k})}{\omega_k} \left\{ h_k - h_p \frac{\vec{p} \cdot \vec{k}}{\vec{p}^2} \right\} \tag{6.1}$$

(all the other Bethe-Salpeter equations follow the same pattern). In conjunction with the partner equation for f_p, the above is one of a homogeneous set of equations, valid only at a particular value of $P_0^2 = M_{\text{PS}}^2$. The standard technique would be to first perform the angular integral involving $\tilde{F}(\vec{p} - \vec{k})$ (in this case, the integral can be performed analytically). Then, the radial integral would be set up on some discrete grid of $\vec{k}^2$ and $\vec{p}^2$ values which results in a matrix form for the coupled equations. One can then use standard matrix methods to determine the eigenvalues (the groundstate meson mass corresponds to the value of P_0^2 where the highest eigenvalue is equal to one) and eigenfunctions. However, in the above case the matrix would involve cancellations of singularities ($\tilde{F}$ is divergent when $\vec{k} = \vec{p}$) between the various terms. To circumvent this would in principle require derivative information about the functions or an infrared regularization of $\tilde{F}$ such as a fictitious mass term. Further, when $\vec{k}$ is in the vicinity of $\vec{p}$, the matrix elements become significantly enhanced. Keeping control over the numerical fidelity in such a situation would become extremely difficult.

As pointed out earlier, the above equation in the chiral limit is very similar to that of the quark gap equation, Eq. (2.13), whose numerical evaluation is well understood [30]. The first step is to change integration variables such that the radial momentum flows through $\tilde{F}$. Denoting $\vec{q} = \vec{p} - \vec{k}$, this then gives

$$h_p = \frac{P_0^2}{4\omega_p^2} f_p + \frac{1}{2} g^2 C_F \int \frac{d\vec{k}\, \tilde{F}_k}{\omega_q} \left\{ h_q - h_p \frac{\vec{p} \cdot \vec{q}}{\vec{p}^2} \right\}. \tag{6.2}$$

Because of the infrared singularity, it is useful to rewrite this equation in the form

$$h_p = \frac{X_p + I_p^1}{1 + I_p^2}, \tag{6.3}$$

where

$$X_p = \frac{P_0^2}{4\omega_p^2} f_p, \qquad I_p^1 = \frac{1}{2} g^2 C_F \int \frac{d\vec{k}\, \tilde{F}_k}{\omega_q} h_q,$$

$$I_p^2 = \frac{1}{2} g^2 C_F \int \frac{d\vec{k}\, \tilde{F}_k}{\omega_q} \frac{\vec{p} \cdot \vec{q}}{\vec{p}^2}. \tag{6.4}$$

This manipulation substitutes the difference of two infrared singular integrals for their ratio, which is numerically less prone to instabilities. Along with the corresponding equation for f_p (manipulated in the same way), we now

introduce a fictitious eigenvalue $\lambda(P_0^2)$ to the left hand sides of both equations, such that we have the form (similarly for f_p)

$$\lambda(P_0^2)h_p = \frac{X_p + I_p^1}{1 + I_p^2}. \tag{6.5}$$

Taking a starting guess for the functions h_p and f_p with the boundary condition $h(\vec{p}^2 \to 0) = 1$, we construct the right hand sides of the equations. This is done by interpolating or extrapolating h_q and f_q within the angular integrals as required, using standard techniques. As will be seen, the functions h_p and f_p are smooth such that this is a numerically safe procedure. The radial integral is performed over a discrete grid of values for $\vec{k}^2$, regulated using an infrared cutoff ε and an ultraviolet cutoff Λ (both with dimensions of [mass]^2). The derived value for h_p at the lowest $\vec{p}^2$ is now compared with the boundary condition (unity) to give the eigenvalue λ. Both derived functions h_p and f_p are then scaled by this value such that the boundary condition is fulfilled. The coupled set of equations is then iterated until convergence of both the functions and the eigenvalue is achieved. Essentially, this procedure is identical to solving an inhomogeneous equation iteratively, but with the lowest grid point value for the function (fixed to unity here) swapped for the eigenvalue (which for the inhomogeneous equation would be trivially absent). The value of P_0^2 for which $\lambda = 1$ is then found.

It is worth pointing out that the numerical procedure described above is certainly not without its limitations. Both integrals I_p^1 and I_p^2 diverge as $1/\sqrt{\varepsilon}$ as $\varepsilon \to 0$, such that the iteration steps are damped (typically by a factor of 10^3) and one must use many steps to achieve a particular tolerance. However, this convergence is stable and easy to implement. If one were to use the difference of the two integrals rather than their ratio, errors in the unknown functions are amplified by such factors and the convergence is highly unstable—one would require an extremely precise starting guess for the functions in order for the iteration to work.

Once the functions h_p and f_p (and in the case of the vector, j_p and g_p too) are found, it is straightforward to obtain the normalization and the leptonic decay constant. In the case of the pseudoscalar meson, h_{PS} can also be found in order to verify the relation Eq. (3.24).

VII. RESULTS

Aside from the quark masses, there is in principle only one free parameter in the truncation scheme studied in this work and this is the string tension σ used in the input function $\tilde{F}$. By setting $\sigma = 1$, all quantities are then (and unless otherwise stated) expressed in appropriate units of σ. To compare with physical quantities, we also give an estimate of the magnitude using the range

$\sqrt{\sigma} \sim \sqrt{\sigma_W} - \sqrt{3\sigma_W} \sim 440 - 762$ MeV as discussed in Sec. II. We use the following numerical parameters throughout this section: the infrared cutoff, $\varepsilon = 10^{-6}$, and the ultraviolet cutoff, $\Lambda = 10^6$. Concerning the value of ε: in Ref. [30] it is seen that the quark mass function converges for $\varepsilon \le 10^{-6}$. We have checked the results here against $\varepsilon = 10^{-5}$ (given the infrared singularities involved, lower values of ε result in significantly more computational effort), and the difference is typically $\le 10^{-3}$ ($\le 3 \times 10^{-3}$) in the pseudoscalar (vector) meson masses and $\le \sim 10^{-4}$ ($\le 3 \times 10^{-3}$) in the pseudoscalar (vector) meson leptonic decay constants. With the typical range of σ values, this tolerance would correspond to ~ 1 MeV. However, notice that for the quark mass function, the difference between results is much smaller for $\varepsilon = 10^{-6}$–10^{-7} than between $\varepsilon = 10^{-5}$–10^{-6} [30]. Thus, we consider the results presented here to be convergent within reasonable limits. The value of Λ is chosen such that the heavy quark masses (up to $m = 10^3$) can be accommodated: with the interaction Eq. (2.3), all results are UV-finite.

Let us begin with the case of (equal mass) chiral quarks. Solving Eq. (2.13) for the quark mass function (as in Ref. [30]) and inserting into Eq. (2.10), the chiral condensate is found to be -0.0123, which with $\sqrt{\sigma} = 440$–762 MeV gives $\langle \bar{q}q \rangle = -(102$–176 MeV$)^3$. While the quark condensate is not a physical quantity, this value is considerably lower than the commonly accepted $\langle \bar{q}q \rangle \sim -(250$ MeV$)^3$. The result here is consistent with previous similar studies, e.g., Refs. [27,29]. Turning to the pseudoscalar meson, this is a special case in that we know analytically that $M_{PS} = 0$. The pseudoscalar leptonic decay constant is found to be $f_{PS} = 0.0260$, which corresponds to $f_{PS} \approx 11$–20 MeV with the above range for $\sqrt{\sigma}$. Again this result agrees with previous studies, e.g., Ref. [27]. Comparing with the physical result for the pion (with our conventions for the normalization), $f_\pi = 92.2$ MeV [36], we see that the pseudoscalar leptonic decay constant for light quarks is almost an order of magnitude too small. Clearly, while chiral symmetry is dynamically broken by the infrared enhanced interaction, the absence of the spatial components of the interaction makes a big difference to the amount of symmetry breaking. The inclusion of more detailed interactions has been recently studied within this context in Ref. [29].

Turning to the chiral quark vector meson, we find that $M_V = 1.553$, or $M_V = 683$–1184 MeV. This has the correct magnitude when compared to the physical result, $M_\rho = 775.5$ MeV [47]. The leptonic decay constant is found to be $f_V = 0.250$, or $f_V = 110$–190 MeV, as compared to $f_\rho = 153$ MeV [38] (with our normalization convention). The calculated vector meson leptonic decay constant is thus also comparable with the magnitude of the physical result, unlike its pseudoscalar counterpart.

Staying with the chiral mesons, the normalized vertex functions h^N, f^N and for the vector, g^N and j^N, are plotted
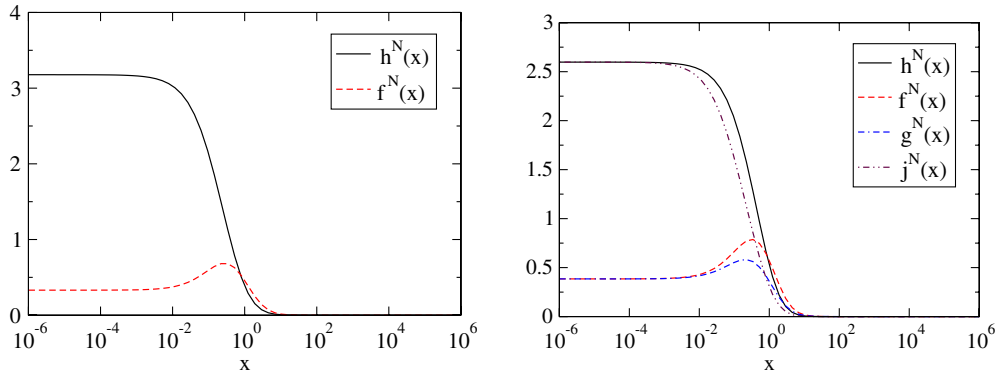
FIG. 3 (color online). [left panel] Pseudoscalar and [right panel] vector normalized vertex functions with (equal) chiral quarks, plotted as a function of $x = \vec{k}^2$. All dimensionfull quantities are in appropriate units of the string tension, σ. See text for details.

in Fig. 3. Recall that these functions are constructed so as to be free from singularities and this is explicitly verified (and has been checked for all combinations of quark masses). The functions are smooth and well-behaved such that the numerical implementation of the angular integrals is indeed justified (see the previous section). In the chiral limit, where $M_{\mathrm{PS}} = 0$, the pseudoscalar function h^N should be identical to the chiral quark mass function, M, up to a constant factor and this has been verified (and serves as a useful numerical check). The vector functions h^N and j^N have a similar form, but with minor differences. The functions f^N (pseudoscalar and vector) and g^N exhibit a bump at around $x = \vec{k}^2 \sim 0.2$–0.5, although this does not seem to have any significance. In the vector case, the pairwise behavior of the functions (f, g) and (h, j) is clearly visible in the IR. As mentioned in the discussion following Eq. (5.16), these pairings occur in the integral expressions for the vector meson Bethe-Salpeter equation: the pairs have the same infrared limit, but at finite momenta j^N and g^N are generally smaller and shifted slightly towards infrared momenta.

Let us now consider mesons with equal mass quarks. The meson masses are plotted in Fig. 4 as a function of the

quark mass, m. One can see that the pseudoscalar meson mass goes approximately like $\sqrt{m}$ in the chiral limit, a clear signal for the dynamical breaking of chiral symmetry and the Goldstone boson nature of the pion. For large quark masses, both meson masses approximate to $2m$ and are degenerate. We have verified that Eq. (3.24) is numerically satisfied (this again serves as a useful numerical check). These results are in explicit agreement with those presented in Ref. [46]. The binding energy, defined as $M_{\mathrm{PS}} - 2m$ (similarly for the vector meson), is also plotted. This provides a more detailed picture of the interaction, since the meson mass is dominated by large quark masses in that limit. One can see that the binding energy is not trivial and decreases for larger quark masses. The degeneracy of the meson masses for heavy quarks is also clearly visible from the binding energy. That the pseudoscalar and vector meson masses are almost equal for equal quark masses above $\mathcal{O}(1)$, means that the mass splitting of charmonium and bottomonium is not present. The leptonic decay constants for the equal quark mass mesons are plotted in Fig. 5. Unlike the meson masses, the leptonic decay constants are only degenerate in the heavy quark limit. For bottomonium, recent lattice results give
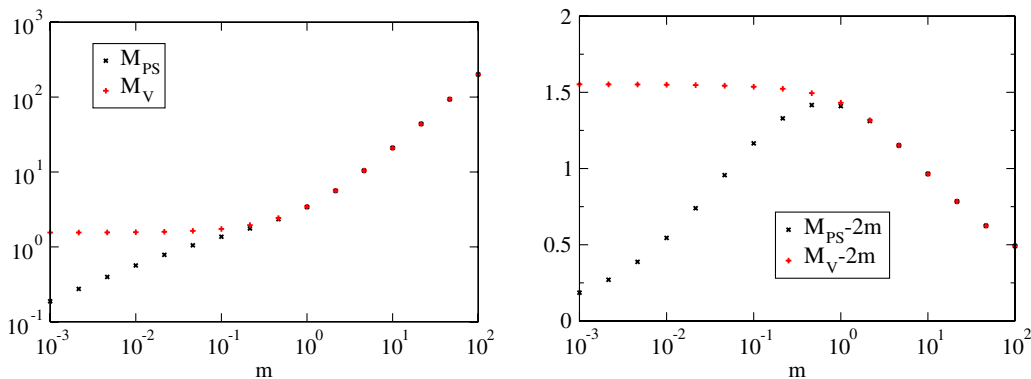

FIG. 4 (color online). Pseudoscalar and vector meson masses [left panel] and binding energies [right panel] with equal mass quarks, plotted as a function of the quark mass. All dimensionfull quantities are in appropriate units of the string tension, σ. See text for details.
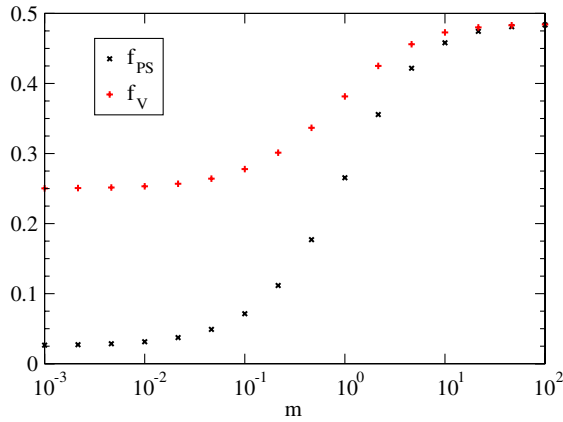
FIG. 5 (color online). Pseudoscalar and vector meson leptonic decay constants with equal mass quarks, plotted as a function of the quark mass. All dimensionfull quantities are in appropriate units of the string tension, σ. See text for details.

$f_{PS} = 472$ MeV [48] (with our conventions); comparing with our results, we get (for the heaviest quark mass) at most $f_{PS} \sim 0.48$, or $f_{PS} \sim 211$–366 MeV. The vector meson result is similar, meaning that both leptonic decay constants are significantly too small, even taking into account the range of values for σ. In the equal quark mass case for large quark masses, the pseudoscalar and vector normalizations become degenerate and go to zero; further, all vertex functions become degenerate.

Finally, let us consider the case where one quark has fixed mass. The meson masses are plotted in Fig. 6 for the case where one quark is fixed to zero bare mass (i.e., $m^- = 0$, $m^+ = m$). In the limit as the other quark mass (m) vanishes, $M_{PS} \sim \sqrt{m}$ (signaling dynamical chiral symmetry breaking), whereas for large masses, $M_{PS} \approx M_V \sim m$ as one would expect. Again, Eq. (3.24) has been numerically verified. As previously, defining a binding energy as $M_{PS} - m$ (similarly for the vector) reveals the interaction in slightly more detail and this is also shown in Fig. 6. The meson masses are degenerate above $m \sim \mathcal{O}(10)$ and the mass-splitting between states is again too small in

this limit. Unlike the case of equal mass quarks we see that the binding energy does not decrease for large quark masses. Turning to the leptonic decay constants, plotted in Fig. 7, the results are again consistently too small. For example, $f_B = 144$ MeV [49,50] (with our convention). Using the input value $\sqrt{\sigma} = \sqrt{\sigma_W}$ and a quark mass of 10, corresponding to a bottom quark of $m = 4.4$ GeV in these units, one has $f_{PS} = 0.168 \sim 74$ MeV, which is clearly too low. On the other hand, taking $\sqrt{\sigma} = \sqrt{3\sigma_W}$ and a quark mass of 4.64, corresponding to $m = 3.5$ GeV, one has the result $f_{PS} = 0.190 \sim 145$ MeV: at first glance this looks like a nice result, but given that the bottom quark mass (in physical units) is realistically too low and that the leptonic decay constant decreases from this point onwards as the quark mass increases (see Fig. 7), the result would be also too small. However, the real interest lies in the heavy quark asymptotic behavior of the leptonic decay constants. In both cases, we should see that the leptonic decay constant decreases as one over the square root of the meson mass and this is explicitly verified in the right panel of Fig. 7, where it is seen that Eqs. (4.31) and (5.22) are fulfilled. Further, it is clear that Eq. (5.24) is satisfied. Looking at the vertex functions in the most extreme case ($m = 10^3$), plotted in Fig. 8, one sees that the functions are all identical. The heavy quark analysis told us that $f^N = h^N$ and $j^N = g^N$; seemingly the pairing of h^N with j^N and f^N with g^N for the vector meson, seen for the equal chiral quark case, also happens here. Thus, the numerical solution to the truncated system does indeed reflect the heavy quark symmetry.

VIII. SUMMARY AND CONCLUSIONS

In this study, a leading order truncation scheme developed in the context of Coulomb gauge Dyson-Schwinger equations [30] has been extended to the Bethe-Salpeter equation framework for quark-antiquark pseudoscalar and vector meson masses and leptonic decay constants, with quark content of arbitrary mass. The leading order Coulomb gauge truncation scheme centers around the
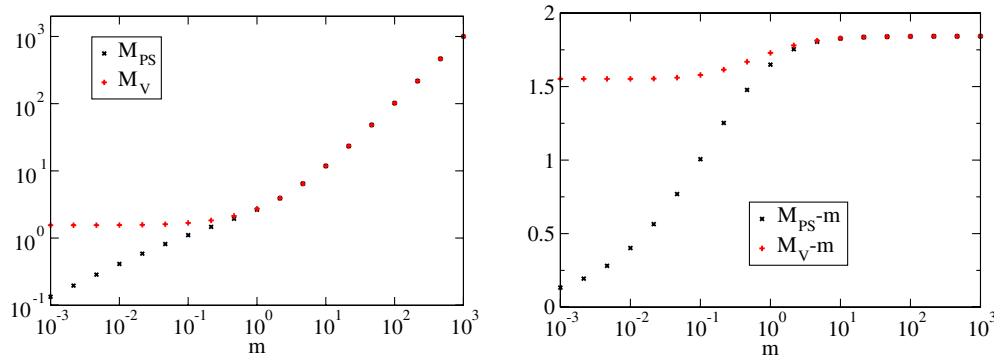

FIG. 6 (color online). Pseudoscalar and vector meson masses [left panel] and binding energies [right panel] with one fixed chiral quark, plotted as a function of the other quark mass. All dimensionfull quantities are in appropriate units of the string tension, σ. See text for details.
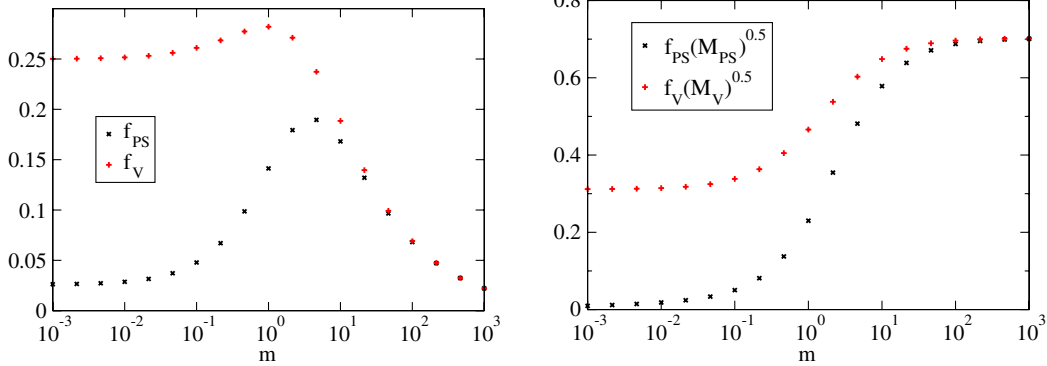
FIG. 7 (color online). Pseudoscalar and vector meson leptonic decay constants [left panel] and $f_{PS}\sqrt{M_{PS}}$, $f_V\sqrt{M_V}$ [right panel] with one fixed chiral quark, plotted as a function of the other quark mass. All dimensionfull quantities are in appropriate units of the string tension, σ. See text for details.

inclusion of an instantaneous and IR singular interaction corresponding to a pure linear rising potential, supplemented by a term arising from the consideration of total color charge conservation. As was briefly discussed, this results in a particular form for the quark gap equation (the Adler-Davis gap equation [27]) for the static quark mass function and for which the divergences cancel and dynamical chiral symmetry breaking is observed. The quark proper two-point function and the self-energy are divergent, reflecting the physical picture that one would require an infinite amount of energy to create a colored object from the vacuum. Further, under this truncation scheme, a connection to the Coulomb gauge rest frame heavy quark limit (in the absence of pure Yang-Mills corrections) [23] can be established.

The connection of the quark propagator to the quark-antiquark (flavor nonsinglet) Bethe-Salpeter equation is well understood via the AXWTI. Following the approach of Ref. [34] (written within the context of the covariant formalism), the necessary framework was briefly reviewed and adapted to the (noncovariant) rest frame Coulomb gauge formalism studied here. The importance and

usefulness of the AXWTI is primarily in that it guarantees that the pion emerges as the massless Goldstone of dynamical chiral symmetry breaking in the chiral limit. Indeed, earlier studies in Coulomb gauge were focused on this aspect [26,28]. However, the AXWTI also applies to arbitrary quark masses, including heavy quarks and allowing a simultaneous analysis of both the chiral and heavy quark limits.

The necessary formalism for calculating the pseudoscalar and vector meson masses and leptonic decay constants was derived. Given the IR singular interaction along with the associated divergence arising from the consideration of total color charge conservation, the overriding concern was the elimination of the IR divergences within the equations. It was seen that this can be explicitly achieved for arbitrary quark mass content and that the pseudoscalar meson is described, within this Coulomb gauge truncation scheme, by two expressly finite functions; the vector meson correspondingly described by four finite functions. In contrast, the Bethe-Salpeter vertices themselves are manifestly divergent. This situation is directly analogous to the case of the quark with a finite
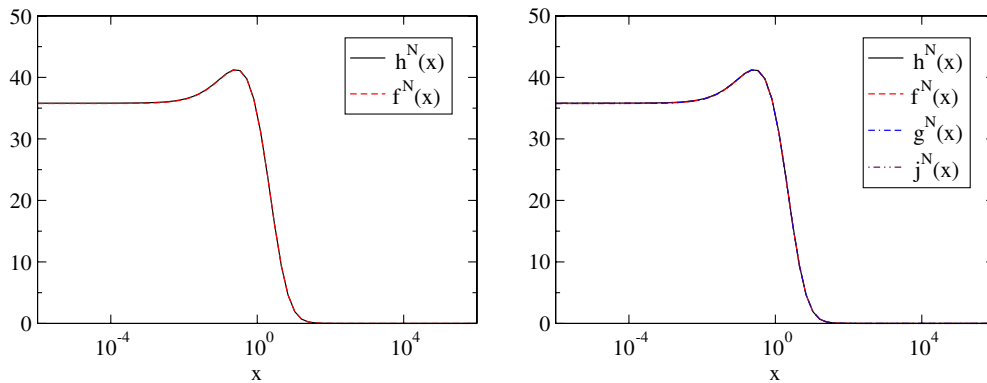

FIG. 8 (color online). [left panel] Pseudoscalar and [right panel] vector normalized vertex functions with one chiral quark and one quark of mass 10^3, plotted as a function of $x = \vec{k}^2$. All dimensionfull quantities are in appropriate units of the string tension, σ. See text for details.

mass function though divergent self-energy. Such cancellations have also been observed in the Coulomb gauge rest frame heavy quark limit for mesons [23], baryons [24], and in the four-point quark Green's functions [25]. The connection to the heavy quark limit was presented and it was shown that the leading order results of heavy quark effective theory [44] are reproduced.

The Bethe-Salpeter equation reduces to a particularly intriguing form within this truncation scheme. As discussed, the expressions, Eqs. (4.15) and (5.15), are a generalization of earlier Coulomb gauge studies of the pseudoscalar meson [26,28] to arbitrary quark masses and extended to include vector mesons. Given the fact that the Bethe-Salpeter equation is constructed from the quark proper two-point function via the AXWTI, it is no surprise that the equations for the pseudoscalar meson have a very similar structure to the quark gap equation [27,30], and directly exhibits the chiral limit properties that one would expect. The dependence on the bound state energy arises in simple fashion and the vector meson appears as an angular momentum excitation of the pseudoscalar. In contrast to covariant gauge studies of the Bethe-Salpeter equation (e.g., Refs. [37–39]) there are no complications, at least within this leading order truncation scheme, arising from the necessity to evaluate the quark propagator dressing functions at complex Euclidean momenta (i.e., the timelike regime) and dealing numerically with possible non-analytic structures (such as in Refs. [40–43]). This allows for an analysis, both analytic and numerical, of mesons with arbitrarily asymmetric quark content.

The derived Bethe-Salpeter equations were solved numerically and results for the pseudoscalar and vector meson masses and their respective leptonic decay constants were presented for arbitrary quark masses. It was explicitly verified that the IR singularities cancel. Clearly visible were both the qualitative pattern of dynamical chiral symmetry breaking and the leading order heavy quark limit. In this respect, the leading order truncation, despite its lack of sophistication is rather successful. Quantitatively, the degree of dynamical mass generation, the mass splitting between the pseudoscalar and vector meson masses, and the leptonic decay constants are all too small (although the vector meson mass and the leptonic decay constant in the chiral limit do have roughly the correct order of magnitude). Having focused on the cancellation of infrared divergences in this study, the coupling of the quarks to the spatial components of the gluon field and the gluon self-interaction have been neglected within the context of the leading order truncation scheme. Clearly, a quantitative comparison to the physical spectrum should include such interactions and this we propose to do in future work.

[1] T. Iritani and H. Suganuma, Phys. Rev. D **83**, 054502 (2011).

[2] A. Voigt, E.-M. Ilgenfritz, M. Muller-Preussker and A. Sternbeck, Phys. Rev. D **78**, 014501 (2008).

[3] Y. Nakagawa, A. Nakamura, T. Saito, and H. Toki, Phys. Rev. D **83**, 114503 (2011).

[4] Y. Nakagawa, A. Nakamura, T. Saito, and H. Toki, Proc. Sci., LAT2009 (2009) 230.

[5] M. Quandt, G. Burgio, S. Chimchinda, and H. Reinhardt, Proc. Sci., CONFINEMENT8 (2008) 066.

[6] A. Cucchieri, A. Maas, and T. Mendes, Mod. Phys. Lett. A **22**, 2429 (2007).

[7] K. Langfeld and L. Moyaerts, Phys. Rev. D **70**, 074507 (2004).

[8] A. Cucchieri and D. Zwanziger, Phys. Rev. D **65**, 014001 (2001).

[9] F. J. Llanes-Estrada and S. R. Cotanch, Nucl. Phys. **A697**, 303 (2002).

[10] F. J. Llanes-Estrada, S. R. Cotanch, A. P. Szczepaniak, and E. S. Swanson, Phys. Rev. C **70**, 035202 (2004).

[11] D. Schutte, Phys. Rev. D **31**, 810 (1985).

[12] A. P. Szczepaniak and E. S. Swanson, Phys. Rev. D **65**, 025012 (2001).

[13] A. P. Szczepaniak, Phys. Rev. D **69**, 074031 (2004).

[14] C. Feuchter and H. Reinhardt, Phys. Rev. D **70**, 105021 (2004); arXiv:hep-th/0402106.

[15] H. Reinhardt and C. Feuchter, Phys. Rev. D **71**, 105002 (2005).

[16] C. E. Fontoura, G. Krein, and V. E. Vizcarra, arXiv:1208.4058.

[17] P. Watson and H. Reinhardt, Phys. Rev. D **75**, 045021 (2007).

[18] P. Watson and H. Reinhardt, Phys. Rev. D **77**, 025030 (2008).

[19] C. Popovici, P. Watson, and H. Reinhardt, Phys. Rev. D **79**, 045006 (2009).

[20] P. Watson and H. Reinhardt, Phys. Rev. D **76**, 125016 (2007).

[21] P. Watson and H. Reinhardt, Eur. Phys. J. C **65**, 567 (2010).

[22] H. Reinhardt and P. Watson, Phys. Rev. D **79**, 045013 (2009).

[23] C. Popovici, P. Watson, and H. Reinhardt, Phys. Rev. D **81**, 105011 (2010).

[24] C. Popovici, P. Watson, and H. Reinhardt, Phys. Rev. D **83**, 025013 (2011).

[25] C. Popovici, P. Watson, and H. Reinhardt, Phys. Rev. D **83**, 125018 (2011).

[26] J. Govaerts, J. E. Mandula, and J. Weyers, Nucl. Phys. **B237**, 59 (1984).

[27] S. L. Adler and A. C. Davis, Nucl. Phys. **B244**, 469 (1984).

[28] R. Alkofer and P. A. Amundsen, Nucl. Phys. **B306**, 305 (1988).

[29] M. Pak and H. Reinhardt, Phys. Lett. B **707**, 566 (2012).

[30] P. Watson and H. Reinhardt, Phys. Rev. D **85**, 025014 (2012).

[31] D. Ebert, T. Feldmann, R. Friedrich, and H. Reinhardt, Nucl. Phys. **B434**, 619 (1995).

[32] A. Cucchieri and D. Zwanziger, Phys. Rev. D **65**, 014002 (2001).

[33] D. Zwanziger, Phys. Rev. Lett. **90**, 102001 (2003).

[34] P. Maris, C. D. Roberts, and P. C. Tandy, Phys. Lett. B **420**, 267 (1998).

[35] P. C. Tandy, Prog. Part. Nucl. Phys. **39**, 117 (1997).

[36] J. L. Rosner and S. Stone, arXiv:1201.2401.

[37] P. Maris and C. D. Roberts, Phys. Rev. C **56**, 3369 (1997).

[38] P. Maris and P. C. Tandy, Phys. Rev. C **60**, 055214 (1999).

[39] R. Alkofer, P. Watson, and H. Weigel, Phys. Rev. D **65**, 094026 (2002).

[40] M. Bhagwat, M. A. Pichowsky, and P. C. Tandy, Phys. Rev. D **67**, 054019 (2003).

[41] C. S. Fischer, P. Watson, and W. Cassing, Phys. Rev. D **72**, 094025 (2005).

[42] A. Krassnigg, Proc. Sci., CONFINEMENT8 (2008) 075.

[43] C. S. Fischer, D. Nickel, and R. Williams, Eur. Phys. J. C **60**, 47 (2009).

[44] M. Neubert, Phys. Rep. **245**, 259 (1994).

[45] K. Langfeld, R. Alkofer, and P. A. Amundsen, Z. Phys. C **42**, 159 (1989).

[46] R. Alkofer, M. Kloker, A. Krassnigg, and R. F. Wagenbrunn, Phys. Rev. Lett. **96**, 022001 (2006).

[47] J. Beringer *et al.* (Particle Data Group Collaboration), Phys. Rev. D **86**, 010001 (2012).

[48] C. McNeile, C. T. H. Davies, E. Follana, K. Hornbostel, and G. P. Lepage, Phys. Rev. D **86**, 074503 (2012).

[49] C.-W. Hwang, Phys. Rev. D **81**, 114024 (2010).

[50] J. L. Rosner and S. Stone, arXiv:0802.1043.